

1 CAMELS-DE: hydro-meteorological time series and attributes for 2 15551582 catchments in Germany

3 Ralf Loritz*¹, Alexander Dolich*¹, Eduardo Acuña Espinoza^{1,A}, Pia Ebeling^{2,A}, Björn Guse^{3,4,A}, Jonas
4 Götte^{5,6,7,A}, Sibylle K. Hassler^{8,A}, Corina Hauffe^{9,A}, Ingo Heidbüchel^{12,10,A}, Jens Kiesel^{3,11,A}, Mirko
5 Mälicke^{1,A}, Hannes Müller-Thomy^{12,A}, Michael Stölzle^{13,A}, Larisa Tarasova^{14,A}

6

7 *equal contribution, A alphabetic order

8 ¹Karlsruhe Institute of Technology (KIT), Institute for Water and Environment, Karlsruhe, Germany

9 ²Helmholtz Centre for Environmental Research - UFZ, Department Hydrogeology, Leipzig, Germany

10 ³Kiel University, Hydrology and Water Resources Management, Kiel, Germany

11 ⁴German Research Centre for Geosciences - GFZ Potsdam, Section Hydrology, Potsdam, Germany

12 ⁵WSL Institute for Snow and Avalanche Research SLF, Davos Dorf, Switzerland

13 ⁶Climate Change, Extremes and Natural Hazards in Alpine Regions Research Center CERC, Davos Dorf

14 ⁷Institute for Atmospheric and Climate Science, ETH Zurich, Zurich, Switzerland

15 ⁸Karlsruhe Institute of Technology (KIT), Institute of Meteorology and Climate Research - Atmospheric Trace Gases and
16 Remote Sensing (IMK-ASF), Karlsruhe, Germany

17 ⁹University of Technology Dresden (TUD), Institute of Hydrology and Meteorology, Dresden, Germany

18 ¹⁰Bayreuth Centre of Ecology and Environmental Research, University of Bayreuth, Bayreuth, Germany

19 ¹¹Stone Environmental, 535 Stone Cutters Way, 05602 Montpelier (VT), USA

20 ¹²Technische Universität Braunschweig, Leichtweiß-Institute for Hydraulic Engineering and Water Resources, Division of
21 Hydrology and River Basin Management, Braunschweig, Germany

22 ¹³Chair of Hydrology, University of Freiburg, Freiburg, Germany, now at: LUBW Landesanstalt für Umwelt (State Agency
23 for Environment), Karlsruhe, Germany

24 ¹⁴Helmholtz Centre for Environmental Research - UFZ, Department Catchment Hydrology, Germany

25

26 *Correspondence to:* Ralf Loritz (Ralf.Loritz@kit.edu) and Alexander Dolich (Alexander.Dolich@kit.edu)

27 **Abstract.** Comprehensive large sample hydrological datasets, particularly the CAMELS datasets (Catchment Attributes and
28 Meteorology for Large-sample Studies), have advanced hydrological research and education in recent years. These datasets
29 integrate extensive hydro-meteorological observations with landscape features, such as geology and
30 land use, across numerous catchments within a national framework. They provide harmonised large sample data for various
31 purposes, such as assessing the impacts of climate change or testing hydrological models on a large number of catchments.

32 Furthermore, these datasets are essential for the rapid progress of data-driven models in hydrology in recent years. Despite
33 Germany's extensive hydrometeorological hydro-meteorological measurement infrastructure, it has lacked a consistent,
34 nationwide hydrological dataset, largely due to its decentralised management across different federal states. This
35 fragmentation has hindered cross-state studies and made the preparation of hydrological data labour-intensive. The
36 introduction of CAMELS-DE represents a step forward in bridging this gap. CAMELS-DE includes 15551582 streamflow
37 gauges with hydro-meteorological time series data covering up to 70 years (median length of 46 years and a minimum length
38 of 10 years), from January 1951 to December 2020. It includes consistent catchment boundaries with areas ranging from 5 to
39 15,000 km² along with detailed catchment attributes covering soil, land cover, hydrogeologic properties and data about
40 human influences. Furthermore, it includes a regionally trained Long-Short Term Memory (LSTM) network and a locally
41 trained conceptual HBV (Hydrologiska Byråns Vattenbalansavdelning) model that were used as quality control and that can
42 be used to fill gaps in discharge data or act as baseline models for the development and testing of new hydrological models.
43 Given the large number of catchments, including numerous relatively small ones (617636 catchments < 100 km²), and the
44 time series length of up to 70 years (156166 catchments with 70 years of discharge data), CAMELS-DE is one of the most
45 comprehensive national CAMELS datasets available and offers new opportunities for research, particularly in studying
46 long-term trends, runoff formation in small catchments and in analysing catchments with strong human influences.

47 1 Introduction

48 The CAMELS (Catchment Attributes and MEteorology for Large-sample Studies) datasets have become a cornerstone
49 within the hydrological community for their comprehensive and consistent integration of hydro- and meteorological data
50 across entire countries, including the USA, UK, Australia, Brazil, Chile, and others (e.g. Addor et al., 2017, Coxon et al.,
51 2020). These datasets combine catchment attributes (e.g. land use, geology, and soil properties), hydrological time series
52 (e.g. water level and discharge), and meteorological time series (e.g. precipitation and temperature) for a multitude of
53 catchments typically within a single country. A distinctive feature of CAMELS datasets is their role as a benchmark for
54 hydrological modelling and large sample analysis, enabling the comparison of hydrological models and the validation of
55 water resources management strategies across diverse landscapes and climates (Brunner et al., 2021). Particularly the
56 CAMELS-US dataset has thereby formed the basis for the on-going rise of machine learning methods in hydrology (e.g
57 Kratzert et al., 2019).

58

59 Despite the widespread adoption and utility of CAMELS datasets in research, teaching, and practical applications globally,
60 Germany with its extensive hydro-meteorological measurement network has no comprehensive and harmonised dataset yet.
61 While there are large sample hydrological datasets that cover either parts of Germany (Klingler et al., 2021), only a fraction
62 of the available national hydrological data (Färber et al., 2023), or focus on catchment water quality and thus cover a lower
63 sampling frequency (Ebeling et al., 2022), the absence of a full CAMELS dataset that includes harmonised, daily,

64 high-quality national hydrological and meteorological data together with catchment attributes and catchment boundaries
65 derived from national and international products limits the potential for comprehensive analyses and advancements in
66 hydrological research and practice. The CAMELS-DE data set addresses this gap (Dolich et al., 2024). CAMELS-DE
67 compiles discharge, water levels, catchment attributes, and catchment boundaries together with a suite of meteorological
68 time series and catchment attributes for ~~1555~~1582 catchments across Germany. Furthermore, ~~it provides discharge~~
69 ~~simulations both from a regional trained Long Short Term Memory (LSTM) network and a local conceptual hydrological~~
70 ~~model with the dataset that can act~~ the dataset includes discharge simulations from two sources: a regionally-trained
71 Long-Short Term Memory (LSTM) network (Hochreiter & Schmidhuber, 1997; Hochreiter, 1998), and a locally trained
72 conceptual HBV model (Hydrologiska Byråns Vattenbalansavdelning, Bergström and Forsman, 1973, Seibert, 2005, Feng et
73 al., 2022). These simulations can serve as a benchmark for future hydrological modelling studies in Germany or be used
74 ~~to help~~ fill missing data gaps in the hydrological time series. Each component of the CAMELS-DE processing pipeline is
75 fully containerized (see section 7), which solves code dependency issues and generally contributes to the traceability,
76 comprehensiveness, and reproducibility of the generation of CAMELS-DE. This study introduces not only a comprehensive
77 dataset but also a suite of tools designed to generate reproducible hydrological datasets from the provided raw data. In the
78 following sections we provide a comprehensive description of all data contained within CAMELS-DE including (1) its
79 source data, (2) how the time series and attributes were produced, and (3) a discussion of the associated limitations and
80 uncertainties. The structure of this paper (and also the corresponding dataset) closely mirrors that of the CAMELS-UK
81 (Coxon et al., 2020) and CAMELS-CH (Höge et al., 2023) studies, ensuring comparability of the datasets while maintaining
82 distinct elements that are not identical but closely related.

83 2 Data sources and providers

84 CAMELS-DE brings together hydrological data, consisting of daily measurements of discharge (m^3/s) and water levels
85 (m), from ~~twelve~~thirteen German federal state agencies, namely the Landesanstalt für Umwelt Baden-Württemberg (LUBW,
86 Nomenclature of Territorial Units for Statistics (NUTS) Level 1: DE1), Bayerisches Landesamt für Umwelt (LfU-Bayern,
87 DE2), Landesamt für Umwelt Brandenburg (LfU-Brandenburg, DE4), Hessisches Landesamt für Naturschutz, Umwelt und
88 Geologie (HLNUG, DE7), Landesamt für Umwelt, Naturschutz und Geologie Mecklenburg-Vorpommern (LUNG MV,
89 DE8), Niedersächsischer Landesbetrieb für Wasserwirtschaft, Küsten- und Naturschutz, Landesamt für Natur (NLWKN,
90 DE9), Umwelt und Verbraucherschutz Nordrhein-Westfalen (LANUV NRW, DEA), Landesamt für Umwelt Rheinland-Pfalz
91 (LUA-Rheinland Pfalz, DEB), Landesamt für Umwelt- und Arbeitsschutz Saarland (LUA, DEC), Landesamt für Umwelt,
92 Landwirtschaft und Geologie Sachsen (LfULG, DED), Landesamt für Umweltschutz Sachsen-Anhalt (LAU, DEE),
93 Landesamt für Landwirtschaft, Umwelt und ländliche Räume Schleswig-Holstein (LLUR, DEF), and Thüringer Landesamt
94 für Umwelt, Bergbau und Naturschutz (TLUBN, DEG). The only federal states not included are the city-states of Bremen,

95 Hamburg, and Berlin, ~~along with the federal state Saarland,~~ which together account for less than ~~1.5~~ 0.6 % of Germany's
96 area, ensuring that the CAMELS-DE dataset remains representative for Germany.

97

98 Meteorological data, specifically precipitation, temperature, relative humidity and radiation, were obtained from the German
99 Weather Service (DWD) from the HYRAS dataset (DWD-HYRAS, 2024). Spatially aggregated catchment attributes were
100 obtained from various sources. From the European Union, we incorporated open-access datasets from Copernicus, the EU's
101 Earth observation program, in particular the Copernicus GLO-30 DEM (Global 30-meter Digital Elevation Model;
102 EU-DEM, 2022) for information about topography and the CORINE Land Cover 2018 dataset (CLC, 2018) for information
103 about land cover. Soil attributes were derived from the global SoilGrids250m dataset (Poggio et al., 2021). Hydrogeological
104 catchment attributes were derived from the “Hydrogeologische Übersichtskarte von Deutschland 1:250.000” (HGM250,
105 2019) provided by the Bundesanstalt für Geowissenschaften und Rohstoffe (BGR) while information about human
106 influences, e.g. dams or weirs, was sourced from Speckhann et al. (2021). ~~All data used in CAMELS-DE is published under~~
107 ~~the open CC BY 4.0 license, allowing free usage as long as proper attribution is provided.~~

108 3 Catchments

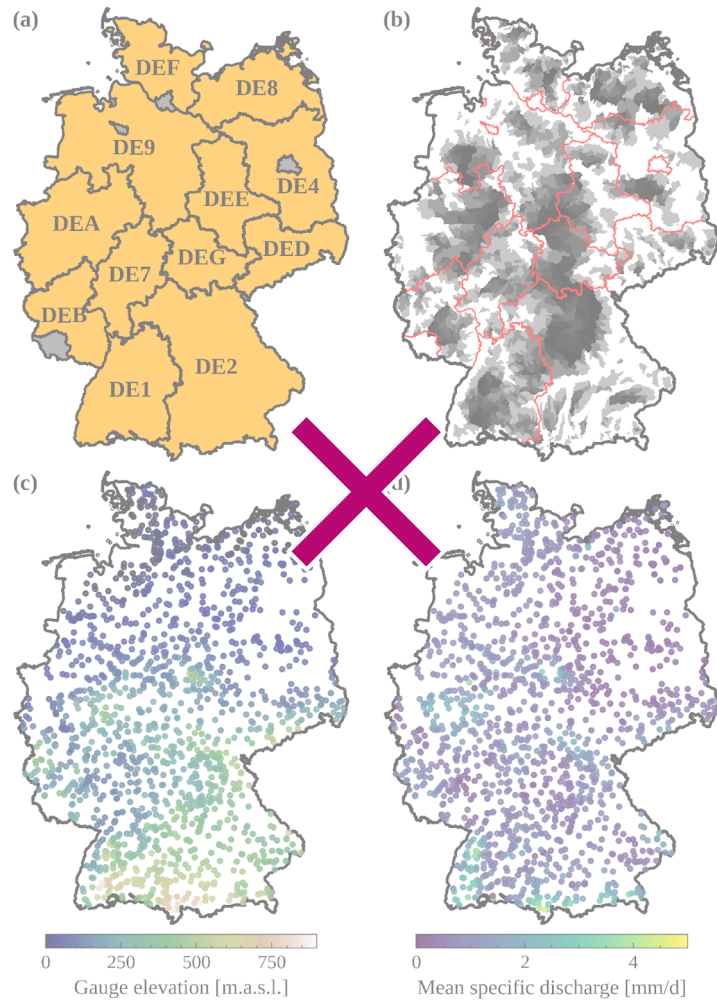
109 For CAMELS-DE, we sourced discharge ($\text{m}^3 \text{s}^{-1}$), water level data (m) and metadata for 2964 gauges and water level stations
110 from the different federal state agencies (see section 2). We created a subset of the data by selecting only measurement
111 stations that contained all required information, such as gauge name, location and catchment area in their metadata ($n = 2700$
112 stations), have at least a total of 10 years of discharge data, which must not necessarily be continuous ($n = 2227$ stations),
113 ~~are have a catchment area~~ larger than 5 km^2 and smaller than $15,000 \text{ km}^2$ ($n = 2586$ stations), ~~are have a catchment area~~
114 located entirely within the borders of Germany ($n = 2298$ stations) and where the derived catchment area does not differ
115 more than 20 % from the reported value by the federal states ($n = 2164$ stations; see section 3.1). These requirements were
116 ~~based on the following reasoning: At least 10 years of discharge data are required to ensure that a sufficient time series~~
117 ~~length is available to perform hydrological modelling and calculate hydrological signatures. These requirements were~~
118 established based on the following rationale: A minimum of 10 years of discharge data is necessary to ensure an adequate
119 time series length for hydrological ~~modeling~~modelling and calculating hydrological signatures. The minimum catchment
120 area of 5 km^2 was ~~selected because some meteorological raster products have a resolution of $5 \times 5 \text{ km}$~~ chosen to match the 1
121 $\times 1 \text{ km}$ resolution of the precipitation raster product, ensuring that multiple raster cells intersect with the catchment
122 boundary. The upper limit was set because catchments larger than $15,000 \text{ km}^2$ are predominantly influenced by human
123 activities and often extend beyond Germany's borders, necessitating their exclusion. The 20 % discrepancy between derived
124 and reported catchment areas was arbitrarily chosen as an acceptable threshold for mass balance errors. This threshold
125 prevents the inclusion of catchments with significantly inaccurate delineations while avoiding the exclusion of too much data
126 (see Fig. 2b). Catchments partially located outside Germany's borders were excluded to avoid complications with

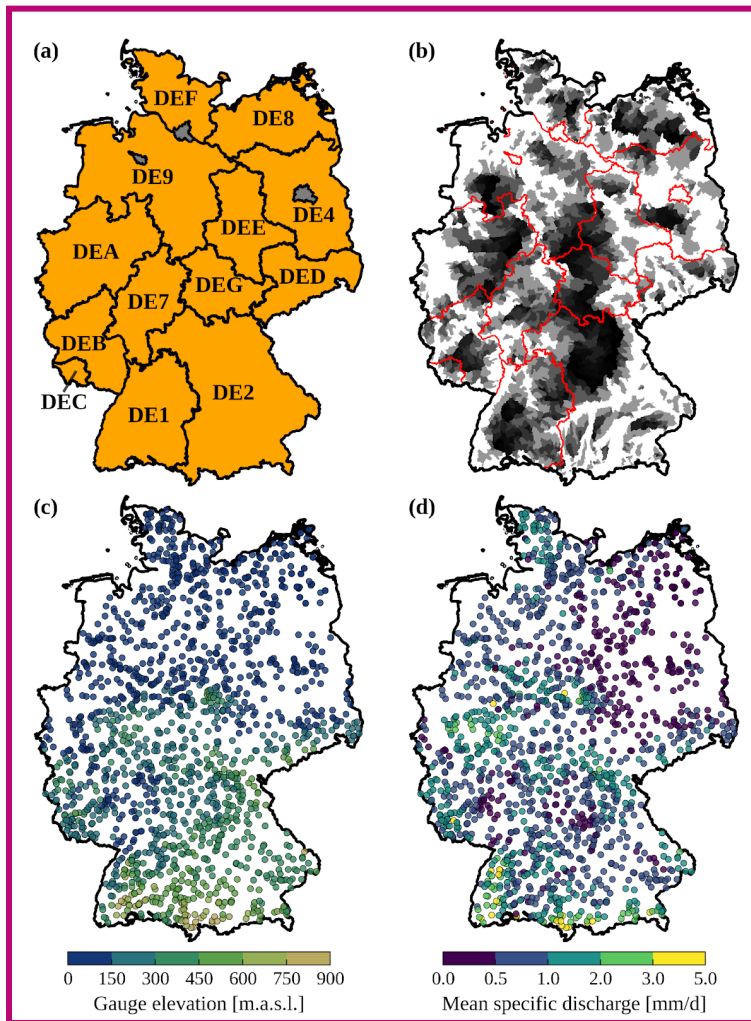
127 cross-border data, especially given the absence of open, high-quality meteorological data from the DWD beyond Germany's
128 national borders from 1951 to 2020. These criteria resulted in a subset of 15551582 gauges for the CAMELS-DE dataset,
129 which provides a reliable representation of hydrological processes in Germany (Fig. 1c, d).

130 3.1 Catchment boundaries

131 Not all state authorities provided official catchment boundaries for their gauging stations, and the methods used by the
132 federal states to derive these boundaries are not uniform and remain unclear. Therefore, we tested two different global
133 catchment datasets, HydroSHEDS (Lehner et al., 2021) and MERIT Hydro (Yamazaki et al., 2019), to derive a consistent set
134 of catchment boundaries across Germany for the CAMELS-DE dataset. For that we compared the catchment areas
135 determined with HydroSHEDS and MERIT Hydro to the catchment areas reported by the state authorities. This comparison
136 was possible because all federal states shared the area of the catchments while not always sharing the actual catchment
137 boundaries. Overall, the comparison revealed that MERIT Hydro has lower errors between the reported and derived
138 catchment areas compared to HydroSHEDS. Among other reasons, this is because MERIT Hydro derives the catchment
139 boundaries directly at the gauge locations provided by the federal states (see section 3.2). The comparison between MERIT
140 Hydro and HydroSHEDS was further supported by extensive manual assessments, involving the visual inspection of
141 numerous catchments to evaluate their shapes and alignments in case the federal state provided the data. Consequently,
142 MERIT Hydro was used for the derivation of catchment boundaries for CAMELS-DE. Note that the derivation of the
143 catchment boundaries is a major source of uncertainty as the meteorological time series and the catchment attributes are
144 dependent on the catchment boundaries. To minimise the uncertainty of the catchment delineation we only included
145 catchments with a deviation of up to 20 percent from the catchment area reported by the federal agencies (Fig. 2b). We report
146 the original catchment area as (area_metadata) and the MERIT-Hydro based area (area) in the table of topographic attributes
147 (Table 2).

148





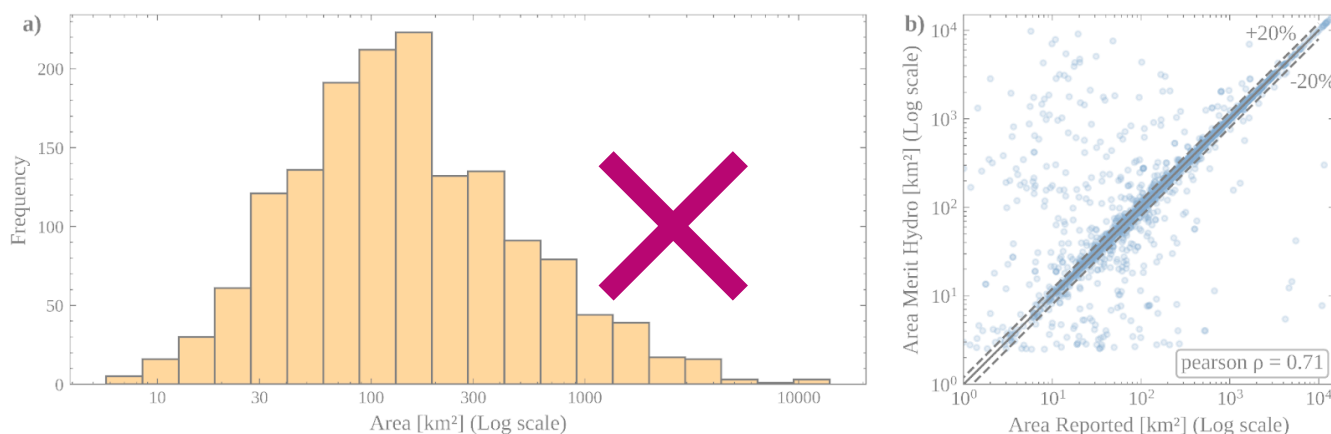
150

151 **Figure 1:** Panel (a) shows the German federal states labelled with their NUTS Level 1 ID as used for the CAMELS-DE gauge IDs. Panel (b) shows all
 152 ~~15551582~~ catchments provided in CAMELS-DE, the geometries of the catchments are shown transparently, so a darker colour means that the geometries of
 153 the catchments in that area overlap; the darker the colour, the higher the density of catchments in that area. Panel (c) and panel (d) show the location of all
 154 ~~15551582~~ gauging stations in CAMELS-DE; in panel (c) the locations are coloured according to the elevation of the gauging station, while in panel (d) the
 155 locations are coloured according to their mean specific discharge value. borders of Germany: © GeoBasis-DE / BKG (VG250, 2023)

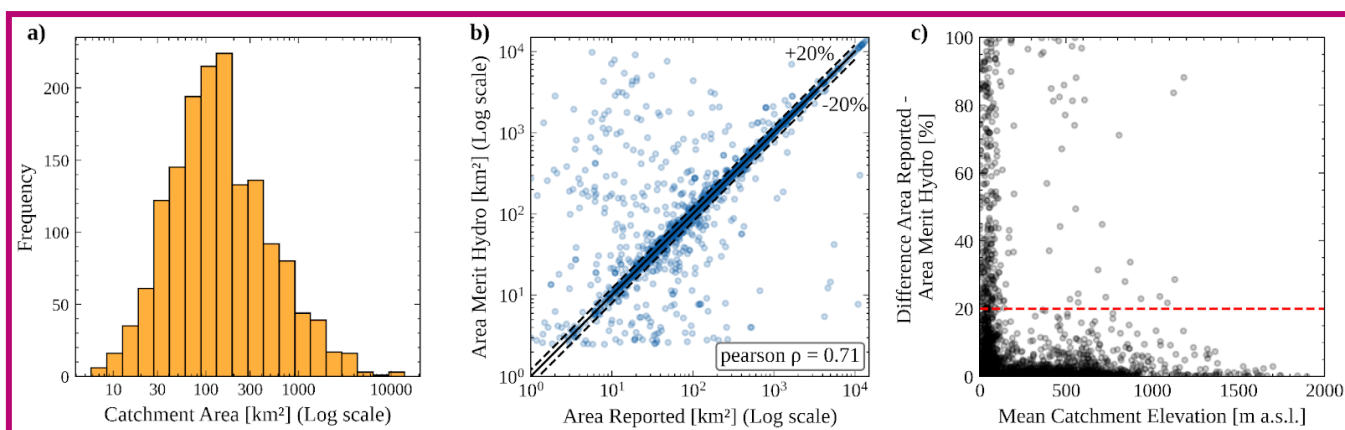
156 3.2 Catchment boundaries derived from MERIT Hydro

157 MERIT (Multi-Error-Removed Improved-Terrain) Hydro was released by Yamazaki et al. (2019); providing a global
 158 hydrography dataset based on the MERIT DEM and various maps of water bodies (e.g. Global 3 arc-second Water Body
 159 Map by Yamazaki et al., 2017). It includes information such as flow direction, flow accumulation, adjusted elevations for
 160 hydrological purposes, and the width of river channels. The delineator.py package (Heberger, 2023) was used to delineate
 161 catchment boundaries. The method automatically derives catchment boundaries from the MERIT Hydro dataset based on the
 162 longitude and latitude of a gauging station and snaps the catchment pour point to the closest stream. Fig. 1b shows all
 163 derived ~~CAMELS-DE~~ catchments using MERIT Hydro within the German borders. The median catchment area within

164 CAMELS-DE is ~~131.3~~129.1 km² (Fig. 2a). Compared to other CAMELS datasets, CAMELS-DE includes a large number of
 165 relatively small catchments with an area of less than 100 km² (i.e. ~~617~~636 catchments, CAMELS-GB: 242 catchments,
 166 CAMELS-US: 142). Uncertainties in catchment delineation arise when comparing areas reported by federal states with those
 167 derived from MERIT Hydro, as shown in Fig. 2b, and these discrepancies are not uniformly distributed across Germany.
 168 They tend to be higher in flat lowland regions with minimal topography (Fig. 2c), particularly in the federal states to the
 169 north and east of Germany. Consequently, a large number of catchments are excluded from the CAMELS-DE dataset in the
 170 northern parts of Germany due to mismatches between reported and estimated areas. In the federal states of Brandenburg
 171 (DE4) and Mecklenburg-Western Pomerania (DE8), for example, we received 447 gauging stations, but given the
 172 uncertainty of the delineation in flat areas, only 277 of them showed a deviation of less than 20 percent from the reported
 173 area. In contrast, in the more mountainous state of Baden-Württemberg (DE1), 225 of 241 catchments met this criterion. As
 174 we report both the catchment areas provided by the federal states and those estimated by MERIT Hydro, the differences
 175 between these two measurements can be used to select or exclude catchments where there are significant uncertainties in the
 176 catchment shape and correspondingly in the derived static and dynamic attributes.



177



178

179 **Figure 2:** Panel (a) shows the distribution of CAMELS-DE catchment areas on a logarithmic scale. Panel (b) shows the accuracy of catchment areas
180 derived using MERIT Hydro compared to the area reported by the federal agencies; the dashed lines indicate ± 20 percent error tolerance that was set for
181 catchment selection.

182 **4 Time series**

183 ~~CAMELS-DE comprises an observation-based and a simulation-based set~~ Panel (c) shows the absolute relative difference between the
184 reported area by the federal states and the MERIT Hydro area against the mean catchment elevation. The red line marks the threshold of 20 percent allowed
185 difference for the inclusion of a catchment in the CAMELS-DE dataset.

186 **4 Time series**

187 CAMELS-DE includes three sets of hydro-meteorological daily time series, as ~~specified in Tab. 1 for a period from 1~~
188 ~~January 1951 to 31 December 2020~~ detailed in Table 1, covering the period from January 1, 1951, to December 31, 2020.
189 These datasets are: (A) observed hydrologic time series (e.g., station discharge and water levels), (B) observed meteorologic
190 time series (e.g., precipitation, temperature, humidity, and radiation), and simulated hydro-meteorologic time series (e.g.,
191 discharge simulated by a LSTM and a HBV model, including estimated evapotranspiration). Note that we do not include any
192 information on evaporation in the non-simulated time series data, as we only include observation-based data here. However,
193 a time series of potential evaporation based on the temperature-based Hargreaves methodology is included in the simulated
194 data (see section 6.2 for more details). However, due to the simplicity of the chosen approach, the potential
195 evapotranspiration time series are highly uncertain, and one should exercise caution when using them.

196

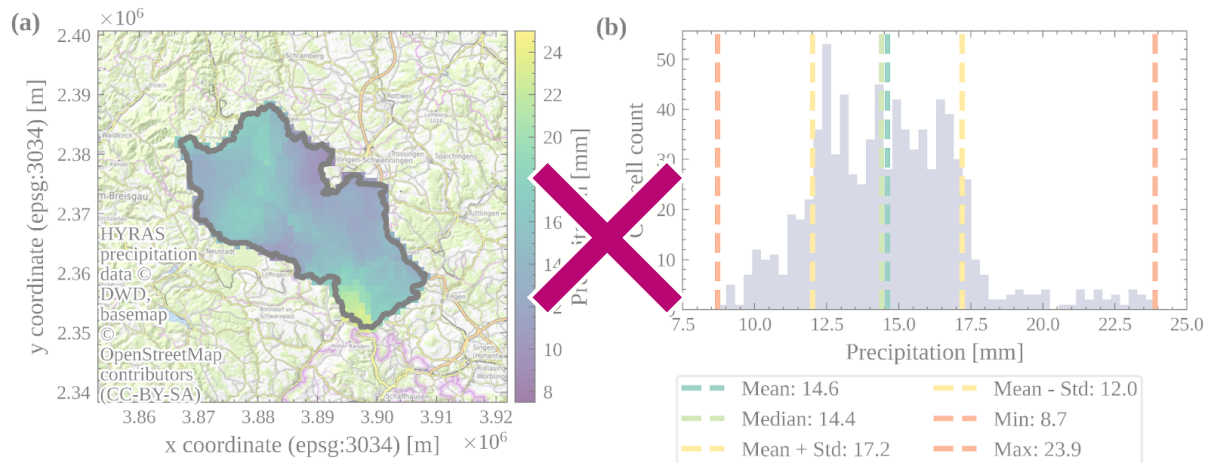
197 All meteorological forcing data within CAMELS-DE are sourced from the ~~Hyras~~HYRAS datasets, which are based on the
198 interpolation of meteorological station data (DWD-HYRAS, 2024). ~~This interpolation was conducted by the DWD (see~~
199 ~~subsection 4.1, 4.2, 4.3).~~ The reliability of these datasets can be compromised by the individual interpolation methods
200 employed (see section 4.1 to 4.3). In addition, inaccuracies in meteorological measurements can introduce uncertainties in
201 the generated grid fields, especially given the extended timescale of 70 years, which may include changes in location and
202 sensor types. Another source of uncertainty is the fact that the number of stations used in the interpolation process varies
203 over time, mirroring changes in the measurement network. For example, the number of stations used for interpolating
204 precipitation data fluctuates, starting at around 4500 in 1951, peaking at approximately 7500 in 2000, and then decreasing to
205 approximately 5000 by 2020. In contrast, the number of stations used for radiation interpolation shows a consistent increase
206 over the years, though the total number remains significantly lower, reaching about 900 stations by 2020. This uncertainty is
207 crucial to consider when comparing data across different years, particularly if the focus is on a single or a few catchments in
208 a certain area. Finally, we use the ‘exact extract’ method, which ensures that raster cells that are only partially covered are
209 treated properly as they are weighted by the proportion of the cell that is covered, i.e. a raster cell that is only 20 % covered
210 by the catchment is only weighted by 20 % when we aggregate to the spatial catchment mean (Fig. 3a illustrates partially
211 covered cells at the catchment boundary). This is particularly important when deriving meteorological data for very small

212 catchment areas. Although this approach also aids in comparing products with different resolutions, it is important to
213 consider that the spatial resolution of the precipitation data, at 1 x 1 km, offers finer detail compared to the 5 x 5 km
214 resolution used for temperature, humidity, and radiation data. This difference is crucial when comparing these datasets within
215 smaller catchments.

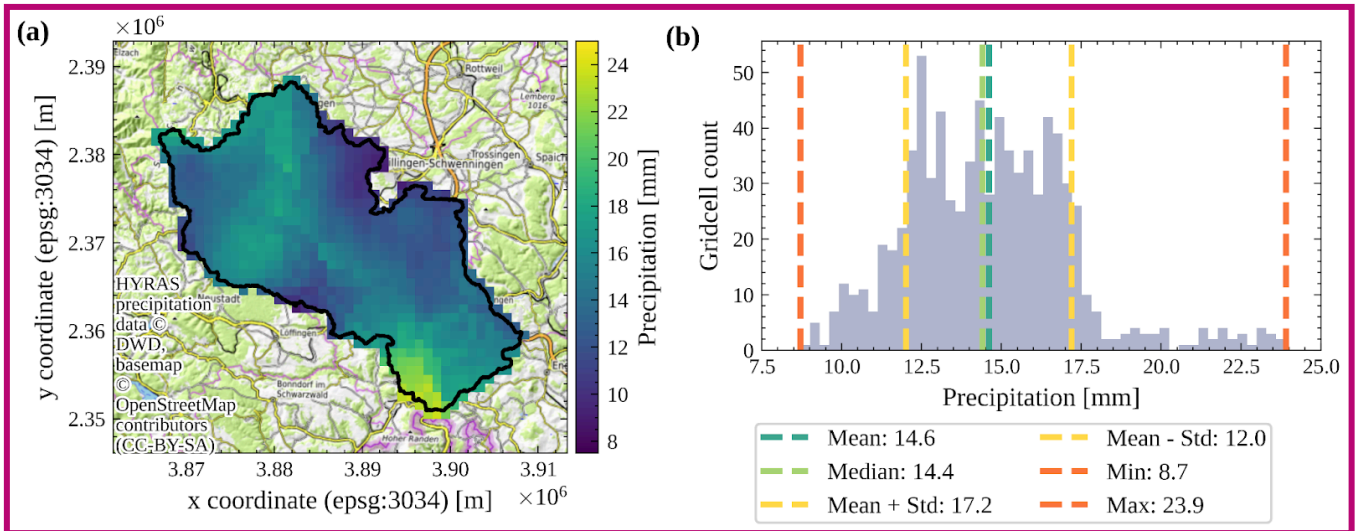
216 4.1 Precipitation

217 CAMELS-DE utilises precipitation data (mm d^{-1}) with daily resolution, sourced from the HYRAS-DE-PRE dataset v5.0
218 (HYRAS-DE-PRE, 2022). We have calculated daily **spatial** minimum, mean, median, maximum, and standard deviation of
219 the rainfall field over the catchment **for each day**. We estimated these statistical measures, rather than just the mean, because
220 this allows us to capture **spatial** variations and patterns that can be crucial for event characterization or rainfall-runoff
221 modelling, as illustrated in Fig. 3. The HYRAS-DE-PRE dataset v5.0 dataset is produced using the REGNIE interpolation
222 method (Rauhe et al., 2013), which employs daily measured values from meteorological stations to generate an interpolated
223 product on a 1x1 km grid. A detailed description of the interpolation method and the related uncertainties can be found in the
224 official data description (HYRAS-DE-PRE, 2022).

225



226



227

228 **Figure 3:** Panel (a) shows the catchment boundaries (black line) of the catchment Kirchen-Hausen in Baden-Württemberg overlaid by a clipped daily
 229 precipitation field from the HYRAS dataset on the date 1951-02-20. Panel (b) shows the spatial distribution of rainfall during the same high precipitation
 230 event as (a) over the catchment on 1951-02-20 and the statistical moments (mean, median, standard deviation, minimum and maximum) derived from the
 231 spatial distribution.

232 4.2 Temperature and relative humidity

233 CAMELS-DE employs daily temperature (°C) and relative humidity (%), derived from the HYRAS-DE-TAS (daily mean
 234 temperature, HYRAS-DE-TAS, 2022), TASMING (daily minimum temperature, HYRAS-DE-TASMIN, 2022), TASMIX
 235 (daily maximum temperature, HYRAS-DE-TASMAX, 2022), and HURS (daily average relative humidity,
 236 HYRAS-DE-HURS, 2022) datasets v5.0, which cover the period from 1951 to 2020 on a 5 km x 5 km grid. This includes the
 237 spatial mean, median, and standard deviation of temperature from HYRAS-DE-TAS, alongside the spatial minimum and
 238 maximum temperatures from TASMING and TASMIX, respectively. Additionally, for humidity, we integrate daily minimum,

239 mean, median, maximum, and standard deviation values across the catchment area. The temperature and humidity data is
240 based on interpolated station values (Razafimaharo et al., 2020). This interpolation method involves a nonlinear regression at
241 each time step, aiming to estimate regional vertical temperature profiles across 13 subregions. These subregions are
242 delineated based on criteria such as weather divides, proximity to the coast, and the extent of north-south variation. A
243 detailed description of the interpolation method and the related uncertainties can be found in the corresponding data
244 descriptions (HYRAS-DE-TAS, (2022); HYRAS-DE-TASMIN, (2022); HYRAS-DE-TASMAX, (2022);
245 HYRAS-DE-HURS, (2022)).

246 4.3 Radiation

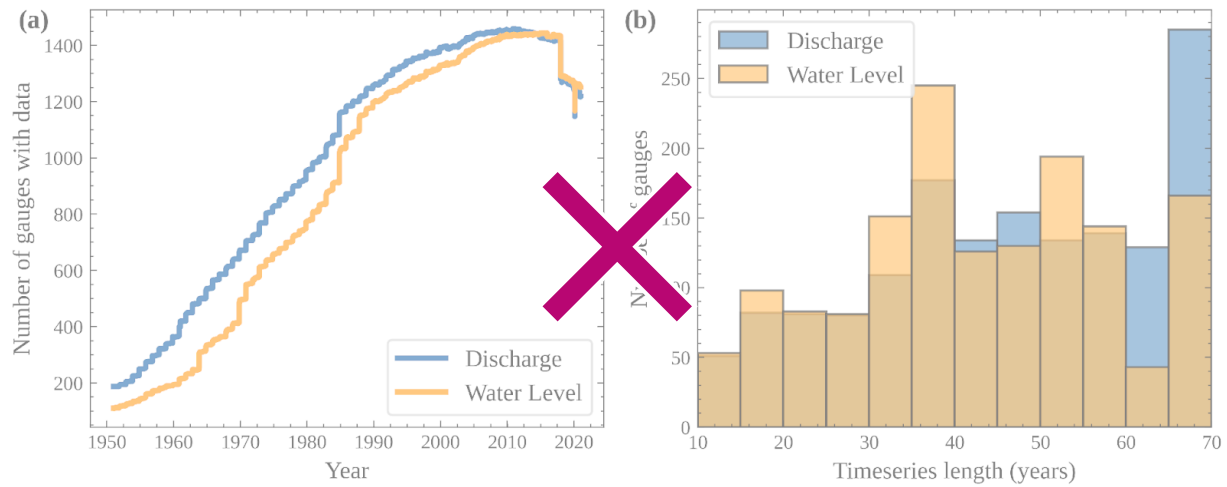
247 The CAMELS-DE dataset utilises daily mean global radiation data (in W m^{-2}) derived from the HYRAS-DE-RSDS datasets
248 v3.0 (HYRAS-DE-RSDS, 2023), that covers a period from 1951 to 2020 with a 5 km x 5 km grid. We have derived daily,
249 spatial minimum, mean, median, maximum, and standard deviation of the radiation field over the catchment for each day.
250 The global radiation (RSDS) dataset integrates station measurement data (including sunshine duration and global radiation),
251 satellite data, and ERA5 data (Muñoz-Sabater et al., 2021). A detailed description of the interpolation method and the related
252 uncertainties can be found in the official data description (HYRAS-DE-RSDS, 2023).

253 4.4 Discharge and water levels

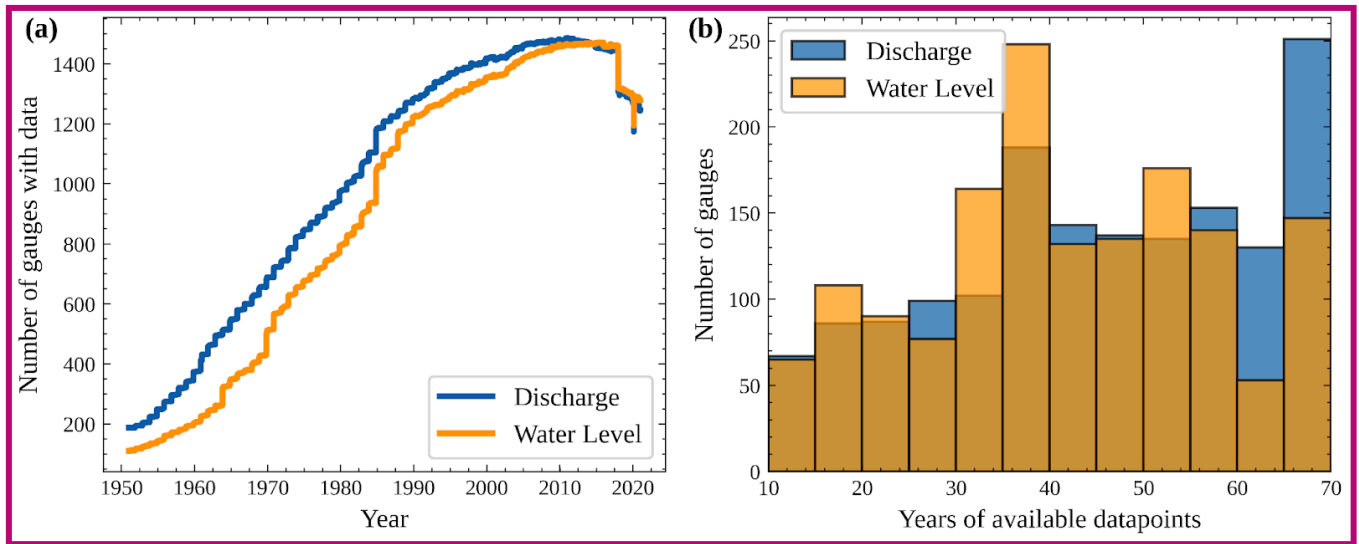
254 Observed discharge and water level data were requested from 13 ~~and delivered from 12 federal~~ state agencies (see section 2)
255 as time series recorded at the gauging stations (Tab. 1). The number of stations with daily discharge data available per year
256 increases in time from 187 on 1 January 1951 to a maximum of ~~1459~~1486 between November 2010 and February 2011 (Fig.
257 4a). The number of stations with water level data is generally lower, starting at 110 stations on 1 January 1951 and reaching a
258 maximum of ~~1444~~1471 stations between March 2015 and December 2015. The time series span a maximum of 70 years,
259 with each measuring station providing at least 10 years of data between January 1951 and December 2020 (Fig. 4b). These
260 10 years do not need to be consecutive but typically are. The median time series length of discharge is 46 years, while the
261 median time series length of water level is 40 years. There is a sharp drop-off in Fig. 4a of 137 stations without data from
262 2017 to 2018 as the provided data from NLWKN (Lower Saxony, DE9) only ~~ranges~~range until the end of 2017. Another
263 anomaly in Fig. 4a is the drop immediately followed by a rise in the year 2020, which is due to the fact that all measuring
264 stations in Rhineland-Palatinate (DEB) show a gap in the discharge data from 10 February 2020 to 15 February 2020 and in
265 the water level data from 13 February 2020 to 15 February 2020. No explanation could be found for this gap. The remaining
266 data after the gap was manually quality controlled by visual inspection of the observed and simulated time series and no
267 reason to exclude this data was found. In total, CAMELS-DE includes 156 stations for which the entire temporal range of 70
268 years of discharge data is available and for which a maximum of 2 percent of the data is missing in this period. There are 85
269 stations where this is the case for water level data.

270 4.5 Discharge and water levels - quality control

271 The quality control of all discharge and water level data was conducted by the respective federal states (quality controlled
272 data was requested). However, the specific methods employed in this quality control are neither the same across the states,
273 nor are they documented in some cases. Typically, quality control entails that a technical clerk has visually inspected the
274 hydrological time series data. To account for this uncertainty we conducted an additional review of all time series data for
275 high negative values and unrealistically high outliers and replaced such data points with ~~NaN~~ not-a-number (NaN) values. We
276 were conservative in these cases and only deleted values that were clear data errors to not remove potential extreme flood
277 events from the time series. This adjustment was necessary in 78 catchments and is documented in the processing pipeline to
278 assure reproducibility. Please note that negative discharge values are still possible in the CAMELS-DE dataset due to the
279 influence of the tide in the northern part of Germany or due to human influences related to water resources management.
280 Moreover, we assessed the hydro-meteorological time series using both a hydrological model and a data-driven model. This
281 analysis helped us identify catchments with weak correlations between meteorological conditions and hydrological responses
282 as well as catchments in which the mass balance is far from being closed. All catchments that exhibited a low model
283 performance of the ~~conceptual~~ HBV model were subjected to manual visual inspection, resulting in the removal of 14
284 catchments (for more details we refer to section 6).



285



286

287 **Figure 4:** Panel (a) shows the number of gauging stations with available discharge (blue) and water level data (orange) in the period from 1951 to 2020,
 288 taking into account data gaps, i.e. the data must actually be available at the respective time. Panel (b) shows ~~the time series length of the discharge and water~~
 289 ~~level observations in CAMELS-DE. Possible gaps in the data are not taken into account in the time series length; in this case, the time series length is the~~
 290 ~~number of years from the first available value to the last available value of a station~~ a histogram of the years of available data points for all measuring
 291 stations, i.e. the length of the time series minus eventual gaps in the time series.

292

293 **Table 1:** Catchment-specific hydro-meteorological variables available as daily time series in CAMELS-DE

Time series class	Time series name	Description	Unit	Data source
Hydrologic time series (1 Jan 1951–31 Dec 2020)	discharge_vol	Catchment Observed catchment discharge calculated from the water level and gauge geometry	$\text{m}^3 \text{s}^{-1}$	Federal state agencies (see section 2)
	discharge_spec	Observed catchment-specific discharge (converted to millimetres per day using	mm d^{-1}	

catchment areas described in section 3.1)

	water_level	Observed daily water level	m	
Meteorologic time series (1 Jan 1951–31 Dec 2020)	precipitation_mean, precipitation_median, precipitation_min, precipitation_max, precipitation_std precipitation_std precipitation_stdev	Observed interpolated spatial mean, median, minimum, maximum and standard deviation of the daily precipitation (original resolution 1x1 km ²)	mm d ⁻¹	German Weather Service HYRAS (DWD-HYRAS, 2024)
	temperature_min	Observed interpolated spatial mean daily minimum temperatures (original resolution 5x5 km ²)	°C	
	temperature_mean	Observed interpolated spatial mean daily mean temperatures (original resolution 5x5 km ²)	°C	
	temperature_max	Observed interpolated spatial mean daily maximum temperatures (original resolution 5x5 km ²)	°C	
	humidity_mean, humidity_median, humidity_min, humidity_max, humidity_std humidity_stddev	Observed interpolated spatial mean, median, minimum, maximum and standard deviation of the daily humidity (original resolution 5x5 km ²)	%	
	radiation_global, radiation_median, radiation_min, radiation_max, radiation_std radiation_global_mean, radiation_global_median, radiation_global_min, radiation_global_max, radiation_global_stddev	Observed interpolated spatial mean, median, minimum, maximum and standard deviation of the global radiation (original resolution 5x5 km ²)	W m ²	
Simulated hydrologic time series (1 Jan 1951–31 Dec 2020)	pet_hargreaves	Daily mean of potential evapotranspiration calculated using the Hargreaves equation	mm d ⁻¹	Regional LSTM model, conceptual HBV and Hargreaves equation for potential evapotranspiration (see section 6, https://github.com/KIT-HYD/Hy2DL/tree/v1.1 , last access: 24 July 2024)
	discharge_vol_obs	Observed volumetric discharge	m ³ s ⁻¹	
	discharge_spec_obs	Observed catchment-specific discharge	mm d ⁻¹	
	discharge_vol_sim_lstm	Volumetric discharge calculated from discharge_spec_sim_lstm and the catchment area	m ³ s ⁻¹	
	discharge_spec_sim_lstm	Catchment-specific discharge simulated with the LSTM (see section 6)	mm d ⁻¹	
	discharge_vol_sim_conceptual ischarge_vol_sim_hbv	Volumetric discharge calculated from discharge_spec_sim_conceptual discharge_spec_sim_hbv and the catchment area	m ³ s ⁻¹	
	discharge_spec_sim_conceptual discharge_spec_sim_hbv	Catchment-specific discharge simulated with the conceptual HBV model (see section 6)	mm d ⁻¹	

simulation_period (training,
validation, testing)

Flag indicating the simulation period in which
the daily value is contained (training, validation,
testing)

294 5 Catchment attributes

295 In addition to the daily time series of hydro-meteorological variables available in CAMELS-DE, the dataset also includes a
296 series of static catchment attributes which are considered time-invariant and include information about topography (section
297 5.1), hydroclimatic signatures (section 5.2) and catchment attributes covering land-cover (section 5.3), soil (section 5.4),
298 hydrogeology (section 5.5) and human influences (section 5.6).

299 5.1 Location and topography

300 For CAMELS-DE, we developed a system of catchment IDs, since the official IDs used by the federal states are inconsistent
301 beyond federal state boundaries. However, the official provider IDs are contained in the topographic attributes of the dataset
302 (Tab. 2). The gauge IDs in CAMELS-DE are based on the NUTS classification, which divides the EU territory hierarchically
303 according to ~~political~~ administrative boundaries. In Germany, the first hierarchical level NUTS 1 provides a code for each
304 federal state (e.g. DE7 for Hessen, DED for Saxony; Fig. 1b). We assign an ID code to each gauge as follows. The ID of
305 each gauge starts with the NUTS 1 code of the corresponding federal state. For each federal state the gauges are coded in
306 arbitrary order starting from 10000 for the first gauge and adding a step of 10 for each following gauge (e.g. DE710000 for
307 the first station in Hessen, DE710010 for the second station, DE710020 for the third station, etc.). This system ensures
308 consistency of the gauge IDs in Germany, and additionally ~~immediately~~ provides the information about the federal state of
309 each gauge. Topographic attributes such as the location (coordinate systems WGS84 and ETRS89), gauge elevation (m) and
310 catchment area (km²) were provided by the federal agencies, the area of the MERIT Hydro catchment is also provided.
311 Additionally we derived the gauge point elevation (m) and basic statistical variables (min, mean, median, 5th and 95th
312 percentile, max) of the catchment elevation (m) from the GLO-30 DEM. CAMELS-DE additionally provides the location of
313 all gauging stations and catchment boundaries as a shape file and a geopackage file.

314 5.2 Climate and hydrology

315 For the CAMELS-DE dataset, we calculated long-term climatic and hydrological signatures in line with the attributes found
316 in CAMELS-CH (covering the period between 1981–2020) and CAMELS-UK (covering the period between 1970–2015)
317 with the difference that we cover the period from 1951–2021 (see Tab. 2). Both types of attributes are calculated based solely
318 on complete hydrological years with respect to the discharge (1 October to 30 September of the following year; again inline
319 with the definition of a hydrological year chosen in CAMELS-UK and CAMELS-CH), with a maximum tolerance of 5 %
320 missing values per hydrological year, ensuring robustness in the data used for analysis. If a specific catchment has discharge

321 data for only a limited number of hydrologic years, we calculate the climatic and hydrological indices for those same years to
322 maintain consistency across all CAMELS datasets and across the climatic and hydrological attributes.

323

324 For each catchment, the hydrologic attributes include values for the mean specific discharge (mm d^{-1}), the runoff ratio, the
325 start and end dates of available discharge data, the percentage of days on which discharge data is available (%), the slope of
326 the flow duration curve between the log-transformed 33rd and 66th percentiles, the ~~day on~~ number of days after which the
327 cumulative discharge since 1 October reaches half of the annual discharge (d), the 5th and 95th quantile of specific discharge
328 (mm d^{-1}) and the frequency of high flow, low flow and zero flow days (d yr^{-1}) together with the average duration of high-flow
329 and low-flow events (d). The climatic attributes are calculated on the basis of the HYRAS meteorological data for each
330 catchment and include mean daily precipitation (mm d^{-1}), the seasonality of precipitation, the fraction of precipitation falling
331 as snow, the frequency of high and low precipitation days (d yr^{-1}), the average duration of high precipitation events and dry
332 periods (d) as well as the season during which most high and low precipitation days occur. The code to estimate the
333 signatures in CAMELS-DE is based on the codes used to derive the signatures for CAMELS-US
334 (<https://github.com/naddor/camels>, last access: 19 July 2024), CAMELS-UK and CAMELS-CH to assure compatibility.

335 5.3 Land cover

336 Land cover in CAMELS-DE is derived from the Corine Land Cover dataset (CLC, 2018) which provides consistent and
337 thematically detailed information on land cover across Europe. The dataset was produced within the frame of the Copernicus
338 Land Monitoring Service referring to land cover / land use status of the year 2018 and is based on the classification of
339 satellite images (other major releases have been published in the years 1990, 2000, 2006, 2012). The CLC dataset from 2018
340 has a spatial resolution of 100 m for raster data. This ensures detailed and consistent land cover information across Europe.
341 CAMELS-DE includes land cover percentages per catchment of the first hierarchical land cover level: artificial surfaces,
342 agricultural areas, forests and semi-natural areas, wetlands and water bodies. The decision to not mix the hierarchical land
343 cover levels ensures that uncertainties in classification due to varying levels of detail are minimised. Catchment shapes and
344 codes to derive land cover classes of lower order or from different releases of CLC in a consistent manner with
345 CAMELS-DE are delivered with the dataset (Dolich, 2024).

346 5.4 Soil

347 Soil attributes for CAMELS-DE are derived from the SoilGrids250m dataset (Poggio et al., 2021), which maps the spatial
348 distribution of soil properties globally at six standard depths. The SoilGrids dataset is generated by training a machine
349 learning model on approximately 240,000 locations worldwide, using over 400 global environmental covariates that describe
350 vegetation, terrain morphology, climate, geology, and hydrology. For CAMELS-DE, we derived the mean values of the soil
351 bulk density, soil organic carbon, volumetric percentage of coarse fragments and proportions of clay, silt and sand for each
352 catchment. The resulting variables are aggregated from the six SoilGrid depths to the depths 0-30 cm, 30-100 cm and

353 100-200 cm by calculating a weighted mean. The accuracy of soil property models, as described by Poggio et al. (2021), is
354 limited by the availability and quality of input data and the assumptions in the modelling process. For instance, discrepancies
355 in how soil data are collected, analysed, and reported by different entities challenge efforts toward data standardisation and
356 harmonisation. However, the relatively high number of observations in Germany reduces this uncertainty to a certain extent.
357 Furthermore, the defined catchment boundaries allow for an assessment of the reported uncertainties within each catchment.
358 If needed the catchment boundaries delivered with CAMELS-DE can be used to calculate the reported uncertainties of
359 SoilGrids within each catchment.

360 5.5 Hydrogeology

361 The hydrogeological attributes for CAMELS-DE are derived from the hydrogeological overview map of Germany on the
362 scale of 1:250,000; "HÜK250" (HGM250, 2019), which describes the hydrogeological characteristics of the upper,
363 large-scale contiguous aquifers in Germany. For CAMELS-DE, the areal percentage of the various HÜK250 classes (see
364 Tab. 2) was calculated for each catchment, whereby the variables of the classes permeability, aquifer media type, cavity type,
365 consolidation, rock type and geochemical rock type sum to 100 percent. Uncertainties in these data may arise from the
366 generalisation required to scale point measurements to a gridded product, which can oversimplify complex hydrogeological
367 features, potentially leading to inaccuracies in the representation of local variations and the spatial distribution of aquifer
368 properties.

369 5.6 Human influence

370 CAMELS-DE includes information on human influences within catchments, primarily focusing on existing dams and
371 reservoirs in Germany. This information is sourced from the inventory of dams in ~~germany~~Germany (Speckhann et al.,
372 2021), which offers detailed data including dam names, locations, associated rivers, years of construction and operation start,
373 crest lengths, dam heights, lake areas, lake volumes, purposes (such as flood control or water supply), dam structure types,
374 and specific building characteristics for 530 dams across Germany. For catchments containing multiple dams, this data is
375 aggregated to provide a comprehensive overview. Specifically, CAMELS-DE includes key information about the dams
376 within each catchment, such as the number of dams, the names of the dams, the rivers where these dams are located, the
377 operational years of the oldest and newest dams, the total area and volume of all dam lakes at full capacity, and the overall
378 purposes of these dams. It is important to note that the "Inventory of Dams in Germany" does not claim to be exhaustive.
379 The absence of recorded dams in this inventory does not necessarily indicate a lack of human influence within a catchment.
380 Nearly all catchments in Germany experience substantial anthropogenic influences, and it is likely that some dams, weirs, or
381 reservoirs (particularly smaller ones) are not documented in the dataset. Another relevant indicator of human influence
382 included in CAMELS-DE is hence the proportion of artificial and agricultural surfaces derived from land cover attributes
383 (see section 5.3).

384 **6 Benchmark LSTMs and conceptual models LSTM and HBV model**

385 CAMELS-DE, in addition to hydro-meteorological observations and catchment attributes, includes results from data-driven
386 and conceptual lumped rainfall-runoff simulations for each catchment. More specifically, these results are derived from a
387 regionally trained LSTM network (trained on all catchments at the same time) and a locally trained lumped ~~conceptual-~~
388 ~~hydrological~~ HBV model (trained at each individual catchment; Bergström and Forsman, 1973, Seibert, 2005, Feng et al.,
389 2022). These models serve three main purposes: (a) they are used to identify catchments where the relationship between
390 meteorological forcing and streamflow is difficult to capture (low model performance), indicating possible strong human
391 influences such as dams or reservoirs, or potential issues with the catchment delineation or the streamflow or meteorological
392 time series; (b) they can serve as a benchmark for future modelling studies based on CAMELS-DE in a sense that the
393 reported performance values and time series can be used as a baseline model and (c) in case of a good model performance
394 can be used to fill missing values of the observed discharge time series. Both models were trained over the period from
395 October 1, 1970, to December 31, 1999, validated from October 1, 1965, to September 30, 1970, and tested from January 1,
396 2000, to December 31, 2020. CAMELS-DE includes the simulated discharges for both models for the entire 70 years (Tab.
397 1), a flag was added to indicate if the corresponding time step was used in training, validation or testing. In the following we
398 explain the model setups and analyse the simulation results in detail. The code of the LSTM model and the ~~conceptual-~~
399 ~~hydrological~~ HBV model were carefully tested and benchmarked (Acuña Espinoza et al., 2024). The codes have been
400 designed to allow easy access and a permalink to the code version used for CAMELS-DE can be found here
401 (<https://github.com/KIT-HYD/Hy2DL/tree/v1.1>, last access: 24 July 2024).

402 **6.1 Setup LSTM model**

403 The LSTM uses mean precipitation, standard deviation of precipitation, mean radiation, mean minimum temperature and
404 mean maximum temperature as dynamic (time varying) input features and specific discharge as a target variable. Static
405 features and hyperparameters were set according to the study of Acuña et al. (2024) with modifications made to (1) an
406 increased hidden size from 64 to 128 and (2) a reduced number of epochs from 30 to 20. The remaining hyperparameters
407 were set as follows: number of hidden layers = 1; learning rate = 0.001; dropout rate = 0.4; batch size = 256; sequence length
408 = 365 days; iterative optimization algorithm = Adam. We use the basin-averaged Nash-Sutcliffe Efficiency (NSE*) loss
409 function proposed by Kratzert et al. (2019) to avoid an imbalance during training due to the higher influence of catchments
410 with a higher runoff generation. ¶

411 **6.2 Setup conceptual models ¶**

412 ~~The lumped conceptual model used in CAMELS-DE is called “simple hydrological model (SHM)” and~~In addition, to the
413 ~~model results (see Tab. 2), we provide the model training epochs of the regional LSTM as part of the CAMELS-DE dataset.~~

414 6.2 Setup HBV model

415 The lumped HBV model used in CAMELS-DE is a variant of the well-known HBV (Hydrologiska Byråns
416 Vattenbalansavdelning; Bergström and Forsman, 1973) model. A detailed description of the model architecture and setup can
417 be found in the studies by ~~Ehret et al. (2020)~~Seibert (2005) and ~~AcuñaFeng et al. (2024)~~. SHM(2022). HBV uses mean
418 precipitation and potential evapotranspiration (E_{pot} ; mm d^{-1}) as inputs. The E_{pot} is calculated using the temperature-based
419 Hargreaves formula, detailed by Adam et al. (2006) and based on earlier work by Droogers and Allen (2002), as explained
420 and cited in Clerc-Schwarzenbach et al. (2024). This variant of the Hargreaves formula resulted in the lowest mass balance
421 error in most catchments with respect to other methods (e.g. Penman, Priestly Taylor) to estimate evapotranspiration and was
422 additionally chosen due to its low data requirements, enabling the utilisation of HYRAS precipitation and temperature data
423 to generate the E_{pot} time series with a limited number of assumptions. The E_{pot} time series are included in CAMELS-DE (Tab.
424 2) for the entire time period of 70 years. In terms of model training/calibration, the SHM was trained individually for each
425 basin using the NSE as a loss function, employing the Differential Evolution Adaptive Metropolis (DREAM; Vrugt, 2016)
426 algorithm as implemented in the SPOTPY (SPOTting model parameters using a ready-made PYthon package, Houska et al.,
427 2015) library. In contrast to the LSTM, the SHM model is mass conserving and hence more sensitive to errors in the
428 catchment delineation that can lead to mass balance errors (see section 3). The difference between the SHM and the LSTM
429 performance can be seen as an indicator either for a strong human influence or for an imprecise catchment delineation as the
430 LSTM can create mass. In addition to the model results (see Tab. 2), we provide the HBV model parameters for each
431 catchment as part of the CAMELS-DE dataset.

432 6.3 Results LSTM and SHM model

433 In this section, we focus our analysis on the LSTM and SHM model in catchments where at least 20 % of the daily data is
434 available during the 30-year training period and 10 % during the testing period, covering a total of ~~1384~~1411 catchments.
435 The median performance of the LSTM, as quantified by the NSE during the testing period, is 0.84 across ~~1384~~1411
436 catchments. Of these, ~~9194~~ catchments have an NSE lower than 0.5 (~~6.66.66~~ % of all catchments), out of which ~~2728~~ have a
437 negative NSE (~~1.951.98~~ % of all catchments). For the ~~9194~~ catchments with NSE below 0.5, most streamflow time series
438 exhibit a low Pearson correlation with daily precipitation (< 0.1) and these catchments are often considerably affected by the
439 construction and/or operation of dams or flood control structures (human influences attributes). Therefore, model
440 performance of the LSTM network can be used to identify catchments that are subject to considerable uncertainties, either
441 due to measurement inaccuracies or significant human influences.

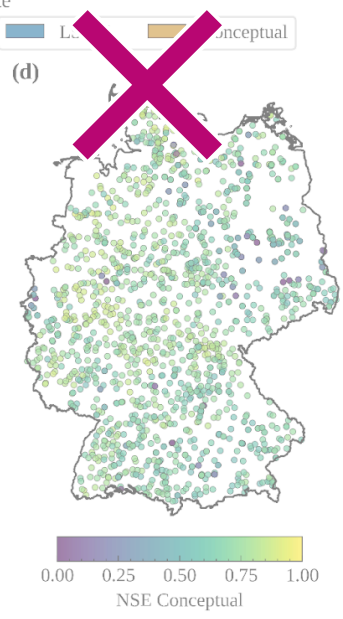
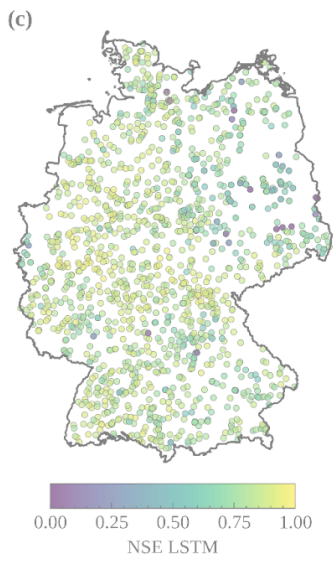
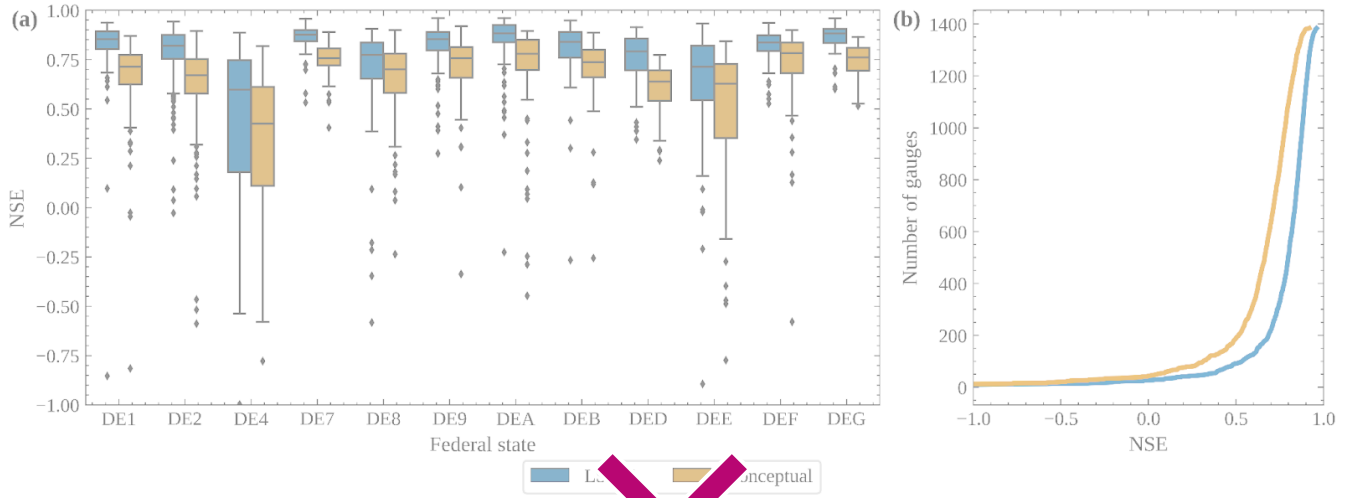
442

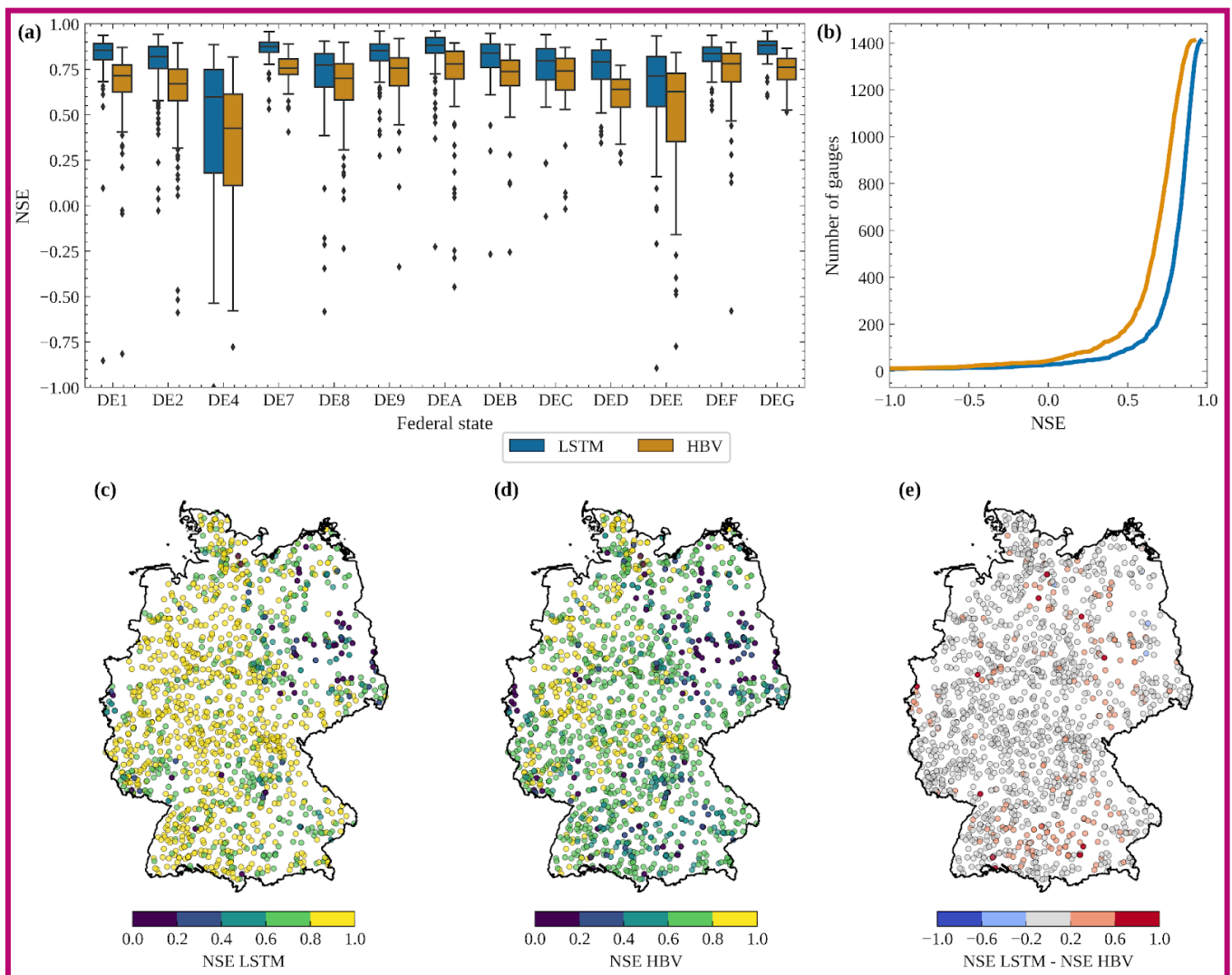
443 Fig. 5a illustrates the performance of the LSTM model across various federal states, with relatively consistent results across
444 the board except for the federal states of Brandenburg (DE4) and Saxony-Anhalt (DEE). In Brandenburg, lowland
445 catchments characterised by sandy soils, considerable groundwater impacts, abundance of natural lakes and human

446 constructed weirs, canals and cross-connections between streams most likely yield a distinctly lower model performance
447 compared to the rest of the German federal states. Besides the federal state of Brandenburg and Saxony-Anhalt the analysis
448 of the LSTMs simulations reveals no clear correlation between the model performance and the topographic attributes (e.g.,
449 area), climatic attributes (e.g., long-term mean precipitation), or hydrological attributes (e.g., long-term mean flow).

450

451 The performance of the ~~conceptual model~~ HBV is with a median NSE of ~~0.71~~ 0.72 lower than that of the LSTM (Fig. 5b). In
452 ~~188~~ 192 catchments (~~13.6~~ 13.61 %) the ~~conceptual model~~ HBV shows a performance below a NSE of 0.5 and in ~~43~~ (3.144
453 (3.12 %) a performance below a NSE of 0. The spatial patterns of performance measured by the NSE are ~~interestingly~~
454 consistent between the LSTM and the ~~conceptual model~~ HBV. In other words, catchments where the LSTM performs well
455 are typically also accurately represented by the ~~conceptual model~~ HBV, and vice versa, as illustrated in Fig. 5e. Catchments
456 in ~~cases the conceptual model~~ which HBV significantly underperforms compared to the LSTM are almost invariably
457 strongly influenced by human-made structures such as dams or weirs, or they are located in areas with uncertain catchment
458 delineation. We propose that the ~~conceptual~~ HBV model, which conserves mass and uses time-invariant parameters, struggles
459 to adapt to dynamic changes in catchment function caused by human activities that result in inaccuracies in water flow and
460 storage due to structures like dams, weirs or due to irrigation or pumping. A hypothesis that requires further testing in the
461 few catchments where this is the case.





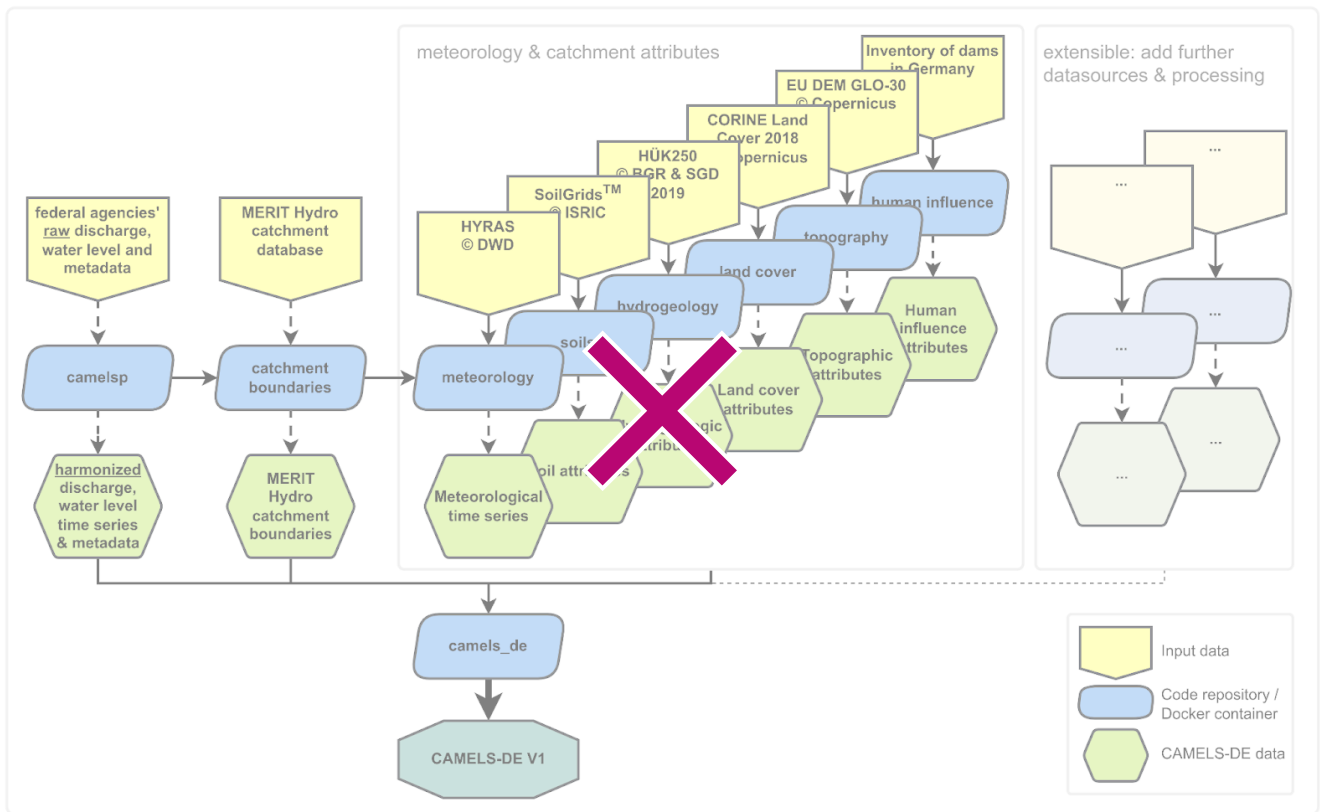
464

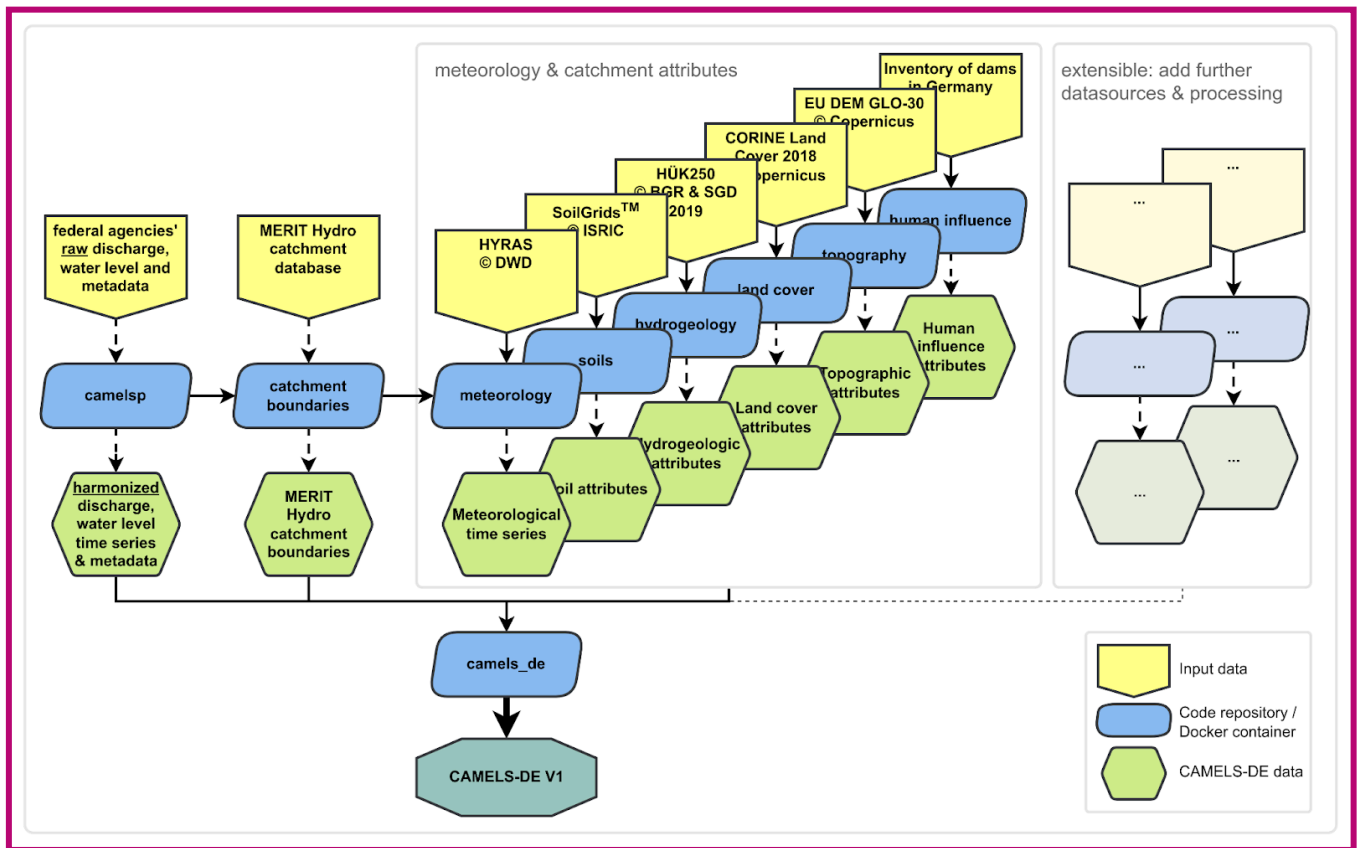
465 **Figure 5:** Panel (a) shows boxplots visualising the distribution of the NSE of the LSTM network (blue) and the **conceptual** HBV model (orange) for each
 466 federal state in Germany for the testing period. Panel (b) shows a cumulative plot of the NSE for the general comparison of the LSTM model and the
 467 **conceptual** HBV model. Panel (c) shows the NSE values of the LSTM for all 1555 gauging stations in Germany, while panel (d) shows the same for the
 468 NSE values of the **conceptual** HBV model. Panel (e) shows the difference between the NSE values of the LSTM and the **conceptual** HBV model for all
 469 gauging stations in Germany, borders of Germany: © GeoBasis-DE / BKG (VG250, 2023)

470 7 Code availability, reproducibility and extensions

471 The processing of CAMELS-DE is structured in a modular manner to enhance the clarity and reproducibility of the
 472 processing pipeline. The CAMELS-DE processing pipeline was published separately with more details and permalinks to the
 473 released repository versions that represent the code state that was used to process and compile CAMELS-DE (Dolich, 2024).

474 For each component of CAMELS-DE, a distinct GitHub repository was established. Within each repository, a dedicated
475 Docker container was developed to process specific input datasets (e.g. HYRAS, GLO-30 DEM). Containerization is
476 particularly well-suited for this project as it ensures that each component of the data processing pipeline runs consistently
477 across different computing environments. This containerization simplifies dependency management, enhances
478 reproducibility, and facilitates the deployment and version control of each processing module. Fig. 6 illustrates the
479 architecture of the processing pipeline, where each blue block represents an individual GitHub repository equipped with a
480 Docker container that processes the yellow input data to produce the green output data. All repositories are uniformly
481 structured, and the accompanying documentation provides detailed descriptions of each repository, guidelines for building
482 and running the Docker containers, including the necessary folder mounts, and instructions for accessing the required input
483 data. In the initial phase of the CAMELS-DE data processing pipeline, raw discharge and water level data, along with station
484 metadata provided by the federal states, are processed and harmonised. Subsequently, MERIT-Hydro catchment boundaries
485 are delineated for each station, a pivotal step since all further datasets depend extensively on these catchment boundaries.
486 Meteorological time series data for these catchments are then processed to compute statistics such as area mean and median.
487 Following this, attributes such as soil properties, hydrogeology, land cover, topography, and human influences are derived for
488 each catchment (see Table 2). In the final stage, all derived data are integrated and formatted according to the established
489 structure of the CAMELS-DE dataset, mirroring the organisational schema of CAMELS-GB or CAMELS-CH.





491

492 **Figure 6:** Diagram of the CAMELS-DE data processing pipeline. Starting with raw discharge and metadata harmonisation, it proceeds to derive
 493 MERIT-Hydro catchment boundaries. Subsequent processing includes meteorological data extraction and aggregation followed by the extraction of various
 494 catchment attributes. In the final step, all extracted data sources are integrated in the structured CAMELS-DE dataset, consistent with CAMELS-GB or
 495 CAMELS-CH (Dolich, 2024).

496 The modular design of the CAMELS-DE processing pipeline enhances its traceability, comprehensibility, and
 497 reproducibility, differing significantly from a monolithic code approach that compiles the entire dataset into a single
 498 repository. This structure not only facilitates the extension of the pipeline to incorporate additional data sources, especially
 499 further catchment attributes, without the need to re-run or rewrite the entire system but also allows for the adaptation of
 500 processing or aggregation methods and the seamless release of updated versions of the CAMELS-DE dataset. The publicly
 501 available Docker containers and the code within them serve not only as a comprehensive guide to understanding the data
 502 processing methods used in CAMELS-DE but also provide a foundation for further data processing using the catchment
 503 geometries included in the dataset. We encourage researchers to enrich CAMELS-DE with additional data sources and
 504 explore ways to enhance the baseline model results. Such contributions are invaluable for continuous improvements and
 505 expansions of the CAMELS-DE dataset, reflecting our commitment to advancing hydrological research and applications
 506 through reproducible science.

507 8 Data availability

508 ~~CAMELS-DE and~~ This manuscript describes the state of version 1.0 of CAMELS-DE, which is freely available at
509 <https://doi.org/10.5281/zenodo.12733968.13837553> (Dolich et al., 2024), accompanied by a comprehensive data description.
510 The code to reproduce CAMELS-DE can be found at <https://doi.org/10.5281/zenodo.12760336> (Dolich, 2024).

511 9 Conclusions

512 CAMELS-DE is a significant step forward in hydrological research for Germany and beyond, offering a comprehensive
513 dataset that spans ~~1555~~1582 catchments with hydro-meteorological daily time series from 1951 to 2020. CAMELS-DE
514 includes detailed catchment delineations and properties, such as reservoir data, land-use, soils, and hydrogeology, which are
515 all vital to analyse and describe the local and regional hydrology of Germany. Furthermore, CAMELS-DE includes
516 simulations from a regionally trained LSTM and locally trained ~~conceptual~~HBV model that can be used either to fill gaps in
517 discharge data in case of good model performance or act as baseline models for the development and testing of new
518 hydrological models. Due to the length of the provided time series of up to 70 years CAMELS-DE opens up new
519 opportunities for investigating long-term hydrological trends or conducting large-sample studies across diverse catchments,
520 including a large number of catchments smaller than 100 km². The dataset's modular design, achieved through the
521 containerization of each processing component, ensures that the data processing is traceable, comprehensible, and
522 reproducible. This approach makes it easier to extend the dataset by incorporating new data sources, adapting processing
523 methods, and releasing updated versions without the need to re-run the entire pipeline. While CAMELS-DE serves as a
524 useful benchmark for large sample hydrology, we invite the scientific community to enrich it with additional data sources
525 and improved methods. In conclusion, CAMELS-DE aims to support a broad range of hydrological research and
526 applications, to foster better understanding and management of water resources in Germany and beyond and to contribute to
527 future global hydrological studies.

528

529 **Author contribution:** RL and MS initiated the CAMELS-DE project. AD prepared and processed data, created most figures
530 and wrote together with RL most of the manuscript. All other authors suggested improvements and made additions to the
531 manuscript, as well as provided data and expertise for specific topics.

532

533 **Competing interests:** At least one of the (co-)authors is a member of the editorial board of Earth System Science Data or
534 Hydrology and Earth System Sciences.

535

536 **Acknowledgment:** We thank the various German institutions for providing observation-based data and sharing their
537 expertise. We are grateful to the Volkswagen Foundation for funding the “CAMELS-DE” project within the framework of

538 the project "Invigorating Hydrological Science and Teaching: Merging Key Legacies with New Concepts and Paradigms"
 539 (ViTamins). We also extend our thanks to ~~NVDI4 Earth~~ **NFDI4Earth**, particularly Jörg Seegert, for their support and
 540 suggestions.

541

542 **Table 2.:** Catchment-specific static attributes available in CAMELS-DE

Attribute class	Attribute name	Description	Unit	Data source
Location and topography	gauge_id	catchment identifier based on the NUTS classification as described in section 5.1 e.g. DE110000, DE110010, ...	–	Federal state agencies (see section 2)
	provider_id	official gauging station ID assigned by the federal states	–	
	gauge_name	gauging station name		
	water_body_name	water body name	–	
	federal_state	federal state in which the measuring station is located		
	gauge_lon	gauging station longitude (EPSG:4326)	°	
	gauge_lat	gauging station latitude (EPSG:4326)	°	
	gauge_easting	gauging station easting (EPSG:3035)	m	
	gauge_northing	gauging station northing (EPSG:3035)	m	
	gauge_elev_metadata	gauging station elevation as given by the federal states	m a.s.l.	
area_metadata	catchment area as given by the federal states	km ²		
	gauge_elev	gauging station elevation derived from the GLO-30 DEM	m a.s.l.	Copernicus GLO-30 DEM (EU-DEM, 2022)
	area	catchment area derived from the MERIT Hydro catchment	km ²	
	elev_mean	mean elevation in the catchment based on the MERIT Hydro geometry	m a.s.l.	
	elev_min	minimum elevation within catchment	m a.s.l.	
	elev_5	5th percentile elevation within catchment	m a.s.l.	
	elev_50	median elevation within catchment	m a.s.l.	

	elev_95	95th percentile elevation within catchment	m a.s.l.	
	elev_max	maximum elevation within catchment	m a.s.l.	
Climate	p_mean	mean daily precipitation long-term mean of daily precipitation from 1951 to 2020	mm d ⁻¹	German Weather Service HYRAS (DWD-HYRAS, 2024)
	p_seasonality	seasonality and timing of precipitation (estimated using sine curves to represent the annual temperature and precipitation cycles, positive (negative) values indicate that precipitation peaks in summer (winter), and values close to zero indicate uniform precipitation throughout the year).	–	
	frac_snow	fraction of precipitation falling as snow, i.e. while mean air temperature is < 0° C	–	
	high_prec_freq	frequency of high-precipitation days (≥ 5 times mean daily precipitation)	d yr ⁻¹	
	high_prec_dur	mean duration of high-precipitation events (number of consecutive days ≥ 5 times mean daily precipitation)	d	
	high_prec_timing	season during which most high-precipitation days occur, e.g. 'jja' for summer. If two seasons register the same number of events a value of NA is given.	season	
	low_prec_freq	frequency of dry days (< 1 mm d ⁻¹)	d yr ⁻¹	
	low_prec_dur	mean duration of dry periods (number of consecutive days < 1 mm d ⁻¹ mean daily precipitation)	d	
	low_prec_timing	season during which most dry season days occur, e.g. 'son' for autumn. If two seasons register the same number of events a value of NA is given.	season	
Hydrology	q_mean	mean daily specific discharge	mm d ⁻¹	Federal state agencies (see section 3.1) and German Weather Service HYRAS (DWD-HYRAS, 2024)
	runoff_ratio	runoff ratio (ratio of mean daily discharge to mean daily precipitation)	–	
	flow_period_start	first date for which daily streamflow data is available	–	
	flow_period_end	last day for which daily streamflow data is available	–	
	flow_perc_complete	percentage of days for which streamflow data is available from Jan 1951–31 Dec 2020	%	
	slope_fdc	slope of the flow duration curve (between the log-transformed 33rd and 66th stream flow percentiles, see Coxon et al.	–	

(2020)

	hfd_mean	mean half-flow date (number of days since 1. Oct at which the cumulative discharge reaches half of the annual discharge)	d	
	Q5	5 % flow quantile (low flow)	mm d ⁻¹	
	Q95	95 % flow quantile (high flow)	mm d ⁻¹	
	high_q_freq	frequency of high-flow days (> 9 times the median daily flow)	d yr ⁻¹	
	high_q_dur	mean duration of high-flow events (number of consecutive days > 9 times the median daily flow)	d	
	low_q_freq	frequency of low-flow days (< 0.2 times the mean daily flow)	d yr ⁻¹	
	low_q_dur	mean duration of low-flow events (number of consecutive days < 0.2 times the mean daily flow)	d	
	zero_q_freq	fraction of days with zero stream flow	–	
Land cover	artificial_surfaces_perc	areal coverage of artificial surfaces	%	CORINE Land Cover 2018 (CLC, 2018)
	agricultural_areas_perc	areal coverage of agricultural areas	%	
	forests_and_seminatural_areas_perc	areal coverage of forests and semi-natural areas	%	
	wetlands_perc	areal coverage of wetlands	%	
	water_bodies_perc	areal coverage of water bodies	%	
Soil	clay_0_30cm_mean clay_30_100cm_mean clay_100_200cm_mean	weight percent of clay particles (< 0.002 mm) in the fine earth fraction at depths 0 - 30 cm, 30 - 100 cm and 100 - 200 cm	wt. %	SoilGrids250m (Poggio et al., 2021)
	silt_0_30cm_mean silt_30_100cm_mean silt_100_200cm_mean	weight percent of silt particles (≥ 0.002 mm and ≤ 0.05/0.063 mm) in the fine earth fraction at depths 0 - 30 cm, 30 - 100 cm and 100 - 200 cm	wt. %	
	sand_0_30cm_mean sand_30_100cm_mean sand_100_200cm_mean	weight percent of sand particles (> 0.05/0.063 mm) at depths 0 - 30 cm, 30 - 100 cm and 100 - 200 cm	wt. %	
	coarse_fragments_0_30cm_mean coarse_fragments_30_100cm_mean coarse_fragments_100_200cm_mean	volumetric fraction of coarse fragments (> 2 mm) at depths 0 - 30 cm, 30 - 100 cm and 100 - 200 cm	vol %	
	soil_organic_carbon_0_30cm_mean soil_organic_carbon_30_100cm_mean	soil organic carbon content in the fine earth fraction at depths 0 - 30 cm, 30 - 100 cm and 100 - 200 cm	g kg ⁻¹	

	mean soil_organic_carbon_100_200cm_ mean			
	bulk_density_0_30cm_mean bulk_density_30_100cm_mean bulk_density_100_200cm_mean	bulk density of the fine earth fraction at depths 0 - 30 cm, 30 - 100 cm and 100 - 200 cm	kg dm ⁻³	
Hydrogeology	aquitard_perc aquifer_perc aquifer_aquitard_mixed_perc	areal coverage of aquifer media type classes	%	HÜK250 © BGR & SGD (Staatlichen Geologischen Dienste) 2019 (HGM, 2019)
	kf_very_high_perc (>1E-2 m s ⁻¹) kf_high_perc (>1E-3 – 1E-2 m s ⁻¹) kf_medium_perc (>1E-4 – 1E-3 m s ⁻¹) kf_moderate_perc (>1E-5 – 1E-4 m s ⁻¹) kf_low_perc (>1E-7 – 1E-5 m s ⁻¹) kf_very_low_perc (>1E-9 - 1E-7 m s ⁻¹) kf_extremely_low_perc (<1E-9 m s ⁻¹) kf_very_high_to_high_perc (>1E-3 m s ⁻¹) kf_medium_to_moderate_perc (>1E-5 – 1E-3 m s ⁻¹) kf_low_to_extremely_low_perc (<1E-5 m s ⁻¹) kf_highly_variable_perc kf_moderate_to_low_perc (>1E-6 – 1E-4 m s ⁻¹)	areal coverage of permeability classes	%	
	cavity_fissure_perc cavity_pores_perc cavity_fissure_karst_perc cavity_fissure_pores_perc	areal coverage of cavity type classes	%	
	consolidation_solid_rock_perc consolidation_unconsolidated_rock_perc	areal coverage of consolidation classes	%	
	rocktype_sediment_perc rocktype_metamorphite_perc rocktype_magmatite_perc	areal coverage of rock type classes	%	
	geochemical_rocktype_silicate_per c geochemical_rocktype_silicate_car bonatic_perc geochemical_rocktype_carbonatic _perc geochemical_rocktype_sulfatic_per c geochemical_rocktype_silicate_or ganic_components_perc geochemical_rocktype_anthropog enically_modified_through_filling	areal coverage of geochemical rock type classes	%	

	geochemical_rocktype_sulfatic_halitic_perc _perc geochemical_rocktype_sulfatic_halitic_perc geochemical_rocktype_halitic_perc			
	waterbody_perc	areal coverage of water body areas according to hydrogeological map	%	
	no_data_perc	percentage of areas with missing data	%	
Human influence	dams_names	names of all dams located in the catchment	–	Inventory of dams in Germany (Speckhann et al., 2021)
	dams_river_names	names of the rivers where the dams are located	–	
	dams_num	number of dams located in the catchment	–	
	dams_year_first	year when the first dam entered operation	–	
	dams_year_last	year when the last dam entered operation	–	
	dams_total_lake_area	total area of all dam lakes at full capacity	km ²	
	dams_total_lake_volume	total volume of all dam lakes at full capacity	Mio m ³	
	dams_purposes	purposes of all the dams in the catchment	–	
Hydrological Simulations	training_perc_complete	percentage of observed specific discharge values in the training period (1970-10-01 – 1999-12-31) that are not NaN	%	Regional LSTM model, conceptual HBV model (see section 6, https://github.com/KIT-HYD/Hy2DL/tree/v1.1 , last access: 24 July 2024)
	validation_perc_complete	percentage of observed specific discharge values in the validation period (1965-10-01 – 1970-09-30) that are not NaN	%	
	testing_perc_complete	percentage of observed specific discharge values in the testing period (2001-10-01 – 2020-12-31) that are not NaN	%	
	NSE_lstm	Nash-Sutcliffe model efficiency coefficient of the LSTM in the testing period	–	
	NSE_conceptual NSE_hbv	Nash-Sutcliffe model efficiency coefficient of the conceptual HBV model in the testing period	–	

543

544 References

545 Acuña Espinoza, E., Loritz, R., Álvarez Chaves, M., Bäuerle, N., and Ehret, U.: To bucket or not to bucket? Analyzing the
546 performance and interpretability of hybrid hydrological models with dynamic parameterization, Hydrology and Earth
547 System Sciences, 28, 2705–2719, <https://doi.org/10.5194/hess-28-2705-2024>, 2024.

- 548 Adam, J. C., Clark, E. A., Lettenmaier, D. P., and Wood, E. F.: Correction of global precipitation products for orographic
549 effects, *J. Clim.*, 19, 15–38, <https://doi.org/10.1175/JCLI3604.1>, 2006.
- 550 Addor, N., Newman, A. J., Mizukami, N., and Clark, M. P.: The CAMELS data set: catchment attributes and meteorology
551 for large-sample studies, *Hydrology and Earth System Sciences*, 21, 5293–5313, <https://doi.org/10.5194/hess-21-5293-2017>,
552 2017.
- 553 Bergström, S. and Forsman, A.: Development of a Conceptual Deterministic Rainfall-runoff Model, *Hydrology Research*, 4,
554 147–170, <https://doi.org/10.2166/nh.1973.0012>, 1973.
- 555 Brunner, M. I., Slater, L., Tallaksen, L. M., and Clark, M.: Challenges in modeling and predicting floods and droughts: A
556 review, *WIREs Water*, 8, <https://doi.org/10.1002/wat2.1520>, 2021.
- 557 CLC: Corine Land Cover <https://doi.org/10.2909/960998c1-1870-4e82-8051-6485205ebbac> (last access: 24 July 2024),
558 2018.
- 559 Clerc-Schwarzenbach, F. M., Selleri, G., Neri, M., Toth, E., van Meerveld, I., and Seibert, J.: HESS Opinions: A few camels
560 or a whole caravan?, *EGUsphere* [preprint], <https://doi.org/10.5194/egusphere-2024-864>, 2024.
- 561 Coxon, G., Addor, N., Bloomfield, J. P., Freer, J., Fry, M., Hannaford, J., Howden, N. J. K., Lane, R., Lewis, M., Robinson,
562 E. L., Wagener, T., and Woods, R.: CAMELS-GB: hydrometeorological time series and landscape attributes for 671
563 catchments in Great Britain, *Earth System Science Data*, 12, 2459–2483, <https://doi.org/10.5194/essd-12-2459-2020>, 2020.
- 564 Dolich, A., Espinoza, E. A., Ebeling, P., Guse, B., Götte, J., Hassler, S., Hauffe, C., Kiesel, J., Heidbüchel, I., Mälicke, M.,
565 Müller-Thomy, H., Stölzle, M., Tarasova, L., & Loritz, R.: CAMELS-DE: hydrometeorological time series and attributes for
566 ~~1555~~1582 catchments in Germany (0.1.01.0.0) [Data set]. Zenodo. <https://doi.org/10.5281/zenodo.12733968>13837553,
567 2024.
- 568 Dolich, A.: CAMELS-DE Processing Pipeline, Zenodo, <https://doi.org/10.5281/zenodo.12760336>13842287, 2024
- 569 Droogers, P. and Allen, R. G.: Estimating reference evapotranspiration under inaccurate data conditions, *Irrig. Drain. Syst.*,
570 16, 33–45, <https://doi.org/10.1023/A:1015508322413>, 2002.
- 571 DWD-HYRAS: <https://www.dwd.de/DE/leistungen/hyras/hyras.html> (last access: 25 March 2024), 2024.
- 572 Ebeling, P., Kumar, R., Lutz, S. R., Nguyen, T., Sarrazin, F., Weber, M., Büttner, O., Attinger, S., and Musolff, A.:
573 QUADICA: water QUALity, DIScharge and Catchment Attributes for large-sample studies in Germany, *Earth System Science*
574 *Data*, 14, 3715–3741, <https://doi.org/10.5194/essd-14-3715-2022>, 2022.

~~575 Ehret, U., van Pruijssen, R., Bortoli, M., Loritz, R., Azmi, E., and Zehe, E.: Adaptive clustering: reducing the computational~~
~~576 costs of distributed (hydrological) modelling by exploiting time-variable similarity among model elements, Hydrology and~~
~~577 Earth System Sciences, 24, 4389–4411, <https://doi.org/10.5194/hess-24-4389-2020>, 2020.~~¶

578 Eiselt, K.-U., Kaspar, F., Mölg, T., Krähenmann, S., Posada, R., and Riede, J. O.: Evaluation of gridding procedures for air
579 temperature over Southern Africa, *Advances in Science and Research*, 14, 163–173,
580 <https://doi.org/10.5194/asr-14-163-2017>, 2017.

581 EU-DEM: Copernicus GLO-30 DEM, <https://doi.org/10.5270/esa-c5d3d65> (last access: 24 July 2024), 2022.

582 Färber, C., Plessow, H., Kratzert, F., Addor, N., Shalev, G., & Looser, U.: GRDC-Caravan: extending the original dataset
583 with data from the Global Runoff Data Centre (0.2) [Data set]. Zenodo. <https://doi.org/10.5281/zenodo.10074416>, 2023.

584 Feng, D., Liu, J., Lawson, K., & Shen, C.: Differentiable, learnable, regionalized process-based models with multiphysical
585 outputs can approach state-of-the-art hydrologic prediction accuracy. *Water Resources Research*, 58, e2022WR032404.
586 <https://doi.org/10.1029/2022WR032404>, 2022.

587 Heberger, M.: delineator.py: Fast, accurate watershed delineation using hybrid vector- and raster-based methods and data
588 from MERIT-Hydro (v1.3). Zenodo. <https://doi.org/10.5281/zenodo.10143149>, 2023.

589 HGM250: Hydrogeological Map of Germany (1:250,000), [https://gdk.gdi-de.org/geonetwork/srv/api/records/](https://gdk.gdi-de.org/geonetwork/srv/api/records/61ac4628-6b62-48c6-89b8-46270819f0d6)
590 [61ac4628-6b62-48c6-89b8-46270819f0d6](https://gdk.gdi-de.org/geonetwork/srv/api/records/61ac4628-6b62-48c6-89b8-46270819f0d6) (last access: 24 July 2024), 2019.

591 Hochreiter, S., & Schmidhuber, J.: Long short-term memory. *Neural Computation*, 9(8), 1735–1780.
592 <https://doi.org/10.1162/neco.1997.9.8.1735>, 1997.

593 Hochreiter, S.: The vanishing gradient problem during learning recurrent neural nets and problem solutions. *International*
594 *Journal of Uncertainty, Fuzziness and Knowledge-Based Systems*, 06(02), 107–116.
595 <https://doi.org/10.1142/s0218488598000094>, 1998.

596 Houska, T., Kraft, P., Chamorro-Chavez, A., and Breuer, L.: SPOTting Model Parameters Using a Ready-Made Python
597 Package, *PLOS ONE*, 10, e0145180, <https://doi.org/10.1371/journal.pone.0145180>, 2015.

598 Höge, M., Kauzlaric, M., Siber, R., Schönenberger, U., Horton, P., Schwanbeck, J., Floriancic, M. G., Viviroli, D., Wilhelm,
599 S., Sikorska-Senoner, A. E., Addor, N., Brunner, M., Pool, S., Zappa, M., and Fenicia, F.: CAMELS-CH:
600 hydro-meteorological time series and landscape attributes for 331 catchments in hydrologic Switzerland, *Earth System*
601 *Science Data*, 15, 5755–5784, <https://doi.org/10.5194/essd-15-5755-2023>, 2023.

602 HYRAS-DE-HURS: Raster data set of daily mean relative humidity in % for Germany - HYRAS-DE-HURS, Version v5.0,
603 [https://opendata.dwd.de/climate_environment/CDC/grids_germany/multi_annual/hyras_de/humidity/DESCRIPTION_GRD_](https://opendata.dwd.de/climate_environment/CDC/grids_germany/multi_annual/hyras_de/humidity/DESCRIPTION_GRD_DEU_P30Y_RH_HYRAS_DE_en.pdf)
604 [DEU_P30Y_RH_HYRAS_DE_en.pdf](https://opendata.dwd.de/climate_environment/CDC/grids_germany/multi_annual/hyras_de/humidity/DESCRIPTION_GRD_DEU_P30Y_RH_HYRAS_DE_en.pdf) (last access: 24 July 2024), 2022.

605 HYRAS-DE-PRE: Raster data set of daily sums of precipitation in mm for Germany - HYRAS-DE-PRE, Version v5.0,
606 [https://opendata.dwd.de/climate_environment/CDC/grids_germany/daily/hyras_de/precipitation/DESCRIPTION_GRD_DE](https://opendata.dwd.de/climate_environment/CDC/grids_germany/daily/hyras_de/precipitation/DESCRIPTION_GRD_DEU_PID_RR_HYRAS-DE_en.pdf)
607 [U_PID_RR_HYRAS-DE_en.pdf](https://opendata.dwd.de/climate_environment/CDC/grids_germany/daily/hyras_de/precipitation/DESCRIPTION_GRD_DEU_PID_RR_HYRAS-DE_en.pdf) (last access: 24 July 2024), 2022.

608 HYRAS-DE-RSDS: Raster data set of daily mean global radiation in W/m² for Germany - HYRAS-DE-RSDS,
609 [https://opendata.dwd.de/climate_environment/CDC/grids_germany/daily/hyras_de/radiation_global/DESCRIPTION_GRD_](https://opendata.dwd.de/climate_environment/CDC/grids_germany/daily/hyras_de/radiation_global/DESCRIPTION_GRD_DEU_PID_RAD_G_HYRAS_DE_en.pdf)
610 [DEU_PID_RAD_G_HYRAS_DE_en.pdf](https://opendata.dwd.de/climate_environment/CDC/grids_germany/daily/hyras_de/radiation_global/DESCRIPTION_GRD_DEU_PID_RAD_G_HYRAS_DE_en.pdf) (last access: 24 July 2024), Version v3.0, 2023.

611 HYRAS-DE-TAS: Raster data set of daily mean temperature in °C for Germany - HYRAS-DE-TAS, Version v5.0,
612 [https://opendata.dwd.de/climate_environment/CDC/grids_germany/daily/hyras_de/air_temperature_mean/DESCRIPTION_](https://opendata.dwd.de/climate_environment/CDC/grids_germany/daily/hyras_de/air_temperature_mean/DESCRIPTION_GRD_DEU_PID_T2M_HYRAS_DE_en.pdf)
613 [GRD_DEU_PID_T2M_HYRAS_DE_en.pdf](https://opendata.dwd.de/climate_environment/CDC/grids_germany/daily/hyras_de/air_temperature_mean/DESCRIPTION_GRD_DEU_PID_T2M_HYRAS_DE_en.pdf) (last access: 24 July 2024), 2022.

614 HYRAS-DE-TASMAX: Raster data set of daily maximum temperature in °C for Germany - HYRAS-DE-TASMAX,
615 Version v5.0,
616 [https://opendata.dwd.de/climate_environment/CDC/grids_germany/monthly/hyras_de/air_temperature_max/DESCRIPTION_](https://opendata.dwd.de/climate_environment/CDC/grids_germany/monthly/hyras_de/air_temperature_max/DESCRIPTION_GRD_DEU_P1M_T2M_X_HYRAS_DE_en.pdf)
617 [GRD_DEU_P1M_T2M_X_HYRAS_DE_en.pdf](https://opendata.dwd.de/climate_environment/CDC/grids_germany/monthly/hyras_de/air_temperature_max/DESCRIPTION_GRD_DEU_P1M_T2M_X_HYRAS_DE_en.pdf) (last access: 24 July 2024), 2022.

618 HYRAS-DE-TASMIN: Raster data set of daily minimum temperature in °C for Germany - HYRAS-DE-TASMIN, Version
619 v5.0,
620 [https://opendata.dwd.de/climate_environment/CDC/grids_germany/daily/hyras_de/air_temperature_min/DESCRIPTION_G](https://opendata.dwd.de/climate_environment/CDC/grids_germany/daily/hyras_de/air_temperature_min/DESCRIPTION_GRD_DEU_PID_T2M_N_HYRAS_DE_en.pdf)
621 [RD_DEU_PID_T2M_N_HYRAS_DE_en.pdf](https://opendata.dwd.de/climate_environment/CDC/grids_germany/daily/hyras_de/air_temperature_min/DESCRIPTION_GRD_DEU_PID_T2M_N_HYRAS_DE_en.pdf) (last access: 24 July 2024), 2022.

622 Klingler, C., Schulz, K., and Herrnegger, M.: LamaH-CE: LARge-SaMple DAta for Hydrology and Environmental Sciences
623 for Central Europe, Earth System Science Data, 13, 4529–4565, <https://doi.org/10.5194/essd-13-4529-2021>, 2021.

624 Kratzert, F., Klotz, D., Shalev, G., Klambauer, G., Hochreiter, S., and Nearing, G.: Towards learning universal, regional, and
625 local hydrological behaviors via machine learning applied to large-sample datasets, Hydrology and Earth System Sciences,
626 23, 5089–5110, <https://doi.org/10.5194/hess-23-5089-2019>, 2019.

627 Lehner, B., Roth, A., Huber, M., Anand, M., Grill, G., Osterkamp, N., Tubbesing, R., Warmedinger, L., and Thieme, M.:
628 HydroSHEDS v2.0 – Refined global river network and catchment delineations from TanDEM-X elevation data, EGU
629 General Assembly 2021, online, 19–30 Apr 2021, EGU21-9277, <https://doi.org/10.5194/egusphere-egu21-9277>, 2021

630 Muñoz-Sabater, J., Dutra, E., Agustí-Panareda, A., Albergel, C., Arduini, G., Balsamo, G., Boussetta, S., Choulga, M.,

631 Harrigan, S., Hersbach, H., Martens, B., Miralles, D. G., Piles, M., Rodríguez-Fernández, N. J., Zsoter, E., Buontempo, C.,
632 and Thépaut, J.-N.: ERA5-Land: a state-of-the-art global reanalysis dataset for land applications, *Earth System Science Data*,
633 13, 4349–4383, <https://doi.org/10.5194/essd-13-4349-2021>, 2021.

634 Poggio, L., de Sousa, L. M., Batjes, N. H., Heuvelink, G. B. M., Kempen, B., Ribeiro, E., and Rossiter, D.: SoilGrids 2.0:
635 producing soil information for the globe with quantified spatial uncertainty, *SOIL*, 7, 217–240,
636 <https://doi.org/10.5194/soil-7-217-2021>, 2021.

637 Rauthe, M., Steiner, H., Riediger, U., Mazurkiewicz, A., and Gratzki, A.: A Central European precipitation climatology Part
638 I: Generation and validation of a high-resolution gridded daily data set (HYRAS), *Meteorologische Zeitschrift*, 22, 235–256,
639 <https://doi.org/10.1127/0941-2948/2013/0436>, 2013.

640 Razafimaharo, C., Krähenmann, S., Höpp, S., Rauthe, M., and Deutschländer, T.: New high-resolution gridded dataset of
641 daily mean, minimum, and maximum temperature and relative humidity for Central Europe (HYRAS), *Theoretical and*
642 *Applied Climatology*, 142, 1531–1553, <https://doi.org/10.1007/s00704-020-03388-w>, 2020.

643 Seibert, J., *HBV Light Version 2. User's Manual*. Department of Physical Geography and Quaternary Geology, Stockholm
644 University, Stockholm, https://www.geo.uzh.ch/dam/jcr:c8afa73c-ac90-478e-a8c7-929eed7b1b62/HBV_manual_2005.pdf
645 (last access: 19. September 2024), 2005

646 Speckhann, G. A., Kreibich, H., and Merz, B.: Inventory of dams in Germany, *Earth System Science Data*, 13, 731–740,
647 <https://doi.org/10.5194/essd-13-731-2021>, 2021.

648 VG250: Verwaltungsgebiete 1:250 000 - Stand 01.01., [https://gdk.gdi-de.org/geonetwork/srv/api/records/
649 93a98c5c-cf03-4a95-bf0a-54001fbf3949](https://gdk.gdi-de.org/geonetwork/srv/api/records/93a98c5c-cf03-4a95-bf0a-54001fbf3949) (last access: 24 July 2024), 2023.

650 Vrugt, J. A.: Markov chain Monte Carlo simulation using the DREAM software package: Theory, concepts, and MATLAB
651 implementation, *Environmental Modelling & Software*, 75, 273–316, <https://doi.org/10.1016/j.envsoft.2015.08.013>,
652 2016.

653 Yamazaki, D., Ikeshima, D., Sosa, J., Bates, P. D., Allen, G. H., and Pavelsky, T. M.: MERIT Hydro: A High-Resolution
654 Global Hydrography Map Based on Latest Topography Dataset, *Water Resources Research*, 55, 5053–5073,
655 <https://doi.org/10.1029/2019wr024873>, 2019.

656 Yamazaki, D., Ikeshima, D., Tawatari, R., Yamaguchi, T., O'Loughlin, F., Neal, J. C., Sampson, C. C., Kanai, S., and Bates,
657 P. D.: A high-accuracy map of global terrain elevations, *Geophysical Research Letters*, 44, 5844–5853,
658 <https://doi.org/10.1002/2017gl072874>, 2017.